UNIVERSITY OF CALIFORNIA, SAN DIEGO

Sodium, potassium-ATPase regulation and calcium signaling during embryonic development

A dissertation submitted in partial satisfaction of the requirements for the degree

Doctor of Philosophy

in

Bioengineering

by

Linda Weishiun Chang

Committee in charge:

Professor Nicholas C. Spitzer, Chair
Professor Shu Chien, Co-Chair
Professor Darwin K. Berg
Professor Wayne R. Giles
Professor Gabriel A. Silva

2008

The Dissertation of Linda Weishiun Chang is approved, and it is acceptable in quality and form for publication on microfilm:

_____

_____

_____

_____
Co-Chair

_____
Chair

University of California, San Diego

2008

TABLE OF CONTENTS

LIST OF ABBREVIATIONS

RT-PCR	reverse transcription polymerase chain reaction
qRT-PCR	quantitative reverse transcription polymerase chain reaction
Na^+, K^+-ATPase	sodium, potassium-adenosine triphosphatase
FXYD	FXYD domain containing ion transport regulator
Olig2	oligodendrocyte transcription factor 2
Olig4	oligodendrocyte transcription factor 4
Orai1	calcium release-activated calcium modulator 1
Notch1	Notch homolog 1
MMR	modified Marc's ringer
DMSO	dimethyl sulfoxide
EDTA	ethylenediaminetetraacetic acid
hCG	human chorionic gonadotropin
MO	morpholino
CMO	control morpholino
DNA	deoxyribonucleic acid
cDNA	complementary deoxyribonucleic acid
RNA	ribonucleic acid
mRNA	messenger ribonucleic acid
SOCE	store-operated calcium entry
SOC	store-operated channel
CRAC	calcium release-activated calcium
bp	base pair
hr	hour
min	minute
sec	second
mm	millimeter
μm	micrometer
nm	nanometer
M	molar
mM	millimolar
μM	micromolar
nM	nanomolar
mg	milligram
μg	microgram
ng	nanogram
L	liter
mL	milliliter
μL	microliter
nL	nanoliter
α	alpha
β	beta

γ	gamma
Hz	hertz
MΩ	megaohm
V_m	membrane potential

LIST OF FIGURES

CHAPTER 3

CHAPTER 4

LIST OF TABLES

CHAPTER 2

ACKNOWLEDGEMENTS

This entire experience would not have been possible without the guidance and support of my advisor, Nick Spitzer. His energy and enthusiasm for scientific research is unparalleled and I am grateful for all of his helpful insights and challenging discussions.

Many members of the Spitzer lab past and present have also helped me immensely throughout the years. In particular, I'd like to thank Brent Miller for helping me with molecular biology and his insightful comments, and Laura Borodinsky for her support and teaching me how to make cultures and calcium image. I also want to thank Davide Dulcis for the fun and often random "nutella-time" conversations in addition to his help with electrophysiology, Xavier Nicol for his assistance with confocal microscopy and the numerous bags of tasty of French croissants, and Kurt Marek for introducing the *Xenopus tropicalis* frogs into our lab.

I thank my family for their love and endless support, especially during the last years of grad school. In particular, I want to thank my mom for always encouraging me to pursue my interests even though she didn't understand what I was doing, or when she did and it grossed her out, my grandma for always making sure that I came back to San Diego with an abundance of food after I went home to visit, and my little brother Arthur for indulging the inner kid in me.

The journey through grad school would have been very isolating without several friends who were able to relate to the frustrations and joys of the entire process. I want to thank Sharon Sann for her friendship, generosity, and entertaining

conversations for keeping me sane. I also want to thank Sara Sternberg Greene for being such a great friend since that first day of college and for the almost daily phone calls we shared over the past 6 years, and Norma Velázquez-Ulloa for the comical discussions and keeping me company during late nights in the lab.

Finally, I'd like to acknowledge the UCSD Moores Cancer Center, the Genomics Core Laboratory at the UCSD Center for AIDS Research (Director, Dr. Christopher Woelk; Grant number, 5P30 AI36214) and the San Diego Veterans Medical Research Foundation for running the qRT-PCR experiments.

The following dissertation is a preprint of "Chang, L.W. and Spitzer, N.C. Spontaneous calcium spike activity in embryonic spinal neurons is driven by developmental expression of the Na^+, K^+-ATPase β3 subunit (in preparation)" of which I am first author.

VITA

2001-2002	Research Assistant Yale University
2002	Bachelor of Science, Magna Cum Laude Yale University
2002-2008	Graduate Student Researcher University of California, San Diego
2003-2005	Teaching Assistant, Department of Bioengineering University of California, San Diego
2005	Master of Science University of California, San Diego
2008	Doctor of Philosophy University of California, San Diego

PUBLICATIONS

Chang, L.W. and Spitzer, N.C. Spontaneous calcium spike activity in embryonic spinal neurons is driven by developmental expression of the Na^+, K^+-ATPase β3 subunit (in preparation).

FIELDS OF STUDY

Major Field: Bioengineering

Studies in Developmental Neurobiology
Professor Nicholas C. Spitzer

ABSTRACT OF THE DISSERTATION

Sodium, potassium-ATPase regulation and calcium signaling during embryonic development

by

Linda Weishiun Chang

Doctor of Philosophy in Bioengineering

University of California, San Diego, 2008

Professor Nicholas C. Spitzer, Chair
Professor Shu Chien, Co-Chair

Different patterns and types of spontaneous electrical activity drive many aspects of neuronal differentiation. In the developing spinal cord, neurons exhibit calcium spikes, which can regulate gene transcription and neurotransmitter specification. The ionic currents necessary for spike production have been described. However, the mechanisms that generate the onset of this activity and the basis of its regulation remain unclear. While signaling molecules appear to act on plasma membrane receptors to trigger calcium spike activity, an autonomous mechanism for

spontaneous calcium spike regulation may exist as well. Here, I show that the β3 subunit of the Na^+, K^+-ATPase is developmentally regulated during a distinct period of embryonic development that coincides with the timing of high calcium spike activity in *Xenopus tropicalis* spinal neurons. Altering temporal expression of β3 with a gene-specific morpholino changes resting membrane potentials and results in suppression of spike activity. Modifying developmental β3 expression also reduces expression of the store-operated channel subunit Orai1, suggesting that the Na^+, K^+-ATPase plays a role in initiating calcium spike activity and regulating calcium homeostasis.

INTRODUCTION

Calcium signaling and electrical activity during development

Calcium signals are vital for many key processes during embryonic development. Abolishing calcium gradients has been shown to affect signaling pathways necessary for normal dorsal-ventral axis formation (Créton et al., 2000; Palma et al., 2001; Webb and Miller, 2003). Calcium gradients are also necessary for left-right asymmetry and disruption of asymmetric calcium signaling causes laterality defects in organ placement (McGrath et al., 2003; Raya et al., 2004; Sarmah et al., 2005). Furthermore, waves of intracellular calcium released from intracellular stores in the dorsal marginal zone are required for convergent extension of embryonic structures. Inhibiting calcium release from these stores with thapsigargin prevents elongation of the notochord and somites during gastrulation (Wallingford et al., 2001).

In the nervous system, fluctuations in intracellular calcium levels attributed to electrical activity manifested by the activation of voltage-gated ion channels and neurotransmitter receptors play important roles in early neuronal development (Spitzer, 2006). During cortical neurogenesis, depolarization of proliferating cells in the ventricular zone by the neurotransmitters gamma-aminobutyric acid (GABA) and glutamate elevates intracellular calcium, and consequently inhibits DNA synthesis (LoTurco et al., 1995). In the developing cerebellum, granule cell migration is also correlated with changes in intracellular calcium levels. These calcium oscillations occur by calcium influx through *N*-methyl-D-aspartate glutamate receptors and N-type calcium channels (Komuro and Rakic, 1992, 1993). When activity is blocked, neuronal migration is inhibited (Komuro and Rakic, 1996).

In addition to proliferation and migration, electrical excitability also affects aspects of neuronal differentiation such neurotransmitter expression. Patterns of electrical activity in cultured primary sensory neurons activate N-type calcium channels, increasing the number of neurons expressing tyrosine-hydroxylase. Eliminating calcium entry through these voltage-gated channels with ω-conotoxin in the presence of electrical stimulation prevents this increase in gene expression at both the mRNA and protein levels (Brosenitsch and Katz, 2001). Likewise, activity regulates the specification of neurotransmitters in embryonic spinal neurons. Imposing different patterns of electrical activity and calcium influx alters transmitter phenotype. By increasing the frequency of calcium oscillations, the number of neurons expressing inhibitory neurotransmitters increases. When activity is suppressed, the number of excitatory neurotransmitters increases (Borodinsky et al., 2004). These examples illustrate some of the many roles for intracellular calcium and electrical activity during neuronal development.

Spontaneous calcium transients in spinal neurons

Several classes of spontaneous calcium transients have been analyzed in growth cones of *Xenopus laevis* spinal neurons. Growth cone transients have been shown to regulate the rate of axon extension (Gomez and Spitzer, 1999; Gu and Spitzer, 1995), substrate-dependent filopodial transients mediate growth cone turning (Gomez et al., 2001), and localized lamellipodial transients facilitate deadhesion and removal of focal complexes (Conklin et al., 2005). These events require calcium

influx through non-voltage-gated calcium channels and all, except for filopodial transients, depend on calcium release from intracellular stores (Conklin et al., 2005; Gomez et al., 2001). Recently, another class of these growth cone calcium transients has been described. Unlike previous types of transients, it relies on calcium influx through the N-type voltage-gated calcium channel $Ca_v2.2$ following interaction with laminin β2 and acts as a stop signal to facilitate appropriate sensory nerve innervation (Sann et al., 2008).

In the soma, spontaneous calcium spikes are action potential-dependent and rely on depolarization-induced calcium influx from voltage-gated calcium channels. These spikes are present early in development prior to synapse formation, can regulate gene transcription, and modulate the specification of excitatory and inhibitory neurotransmitters, as described previously (Borodinsky et al., 2004; Gu and Spitzer, 1995). The ionic currents of these calcium-dependent action potentials have been identified and spikes likely result from initial activation of low voltage-activated (LVA) calcium T currents, which brings the membrane potential closer to threshold to activate sodium and high voltage-activated (HVA) calcium currents (Gu and Spitzer, 1993). This triggers an influx of calcium that ultimately leads to calcium-induced calcium release from intracellular stores (Holliday et al., 1991). Over time, repolarization of the membrane subsequently eliminates the calcium component of the action potential through activation of outward potassium currents (Lockery and Spitzer, 1992; O'Dowd et al., 1988).

Though the currents responsible for driving calcium-dependent action potentials have been identified, the developmental events responsible for eliciting the onset of this spontaneous activity remain to be determined. Recent evidence suggests that GABA and glutamate, which are present early in development, bind to metabotropic $GABA_B$ and group III metabotropic glutamate receptors to drive calcium spike activity by activating protein kinase signaling pathways (Root et al., 2008). However, spikes also occur in sparsely plated cultured neurons that do not contact other cells, suggesting that an autonomous mechanism influences the initiation of spike activity as well. This may include developmental regulation of other ion channels or transporters upstream of spontaneous calcium spiking, which could trigger the depolarization necessary to initiate this phenomenon. In the following study, I propose that genetically programmed developmental expression of a Na^+, K^+-ATPase subunit gene prior to the onset of calcium spiking is necessary for regulating the appearance of this activity.

Functional components of the Na^+, K^+-ATPase

The Na^+, K^+-ATPase is a heteromeric electrogenic pump that utilizes energy from ATP hydrolysis to pump three sodium ions out of and two potassium ions into eukaryotic cells, and is vital to maintaining electrical and chemical gradients across the plasma membrane. Both an α and β subunit are needed to produce a functional enzyme capable of ion transport (Noguchi et al., 1987). It is widely accepted that the pump primarily consists of an $\alpha\beta$ dimer, although higher order oligomers of $\alpha\beta$

protomers may exist (Blanco et al., 1994; Donnet et al., 2001; Linnertz et al., 1998; Tsuda et al., 1998). Four α and three β isoforms have been characterized. The α subunit is a ~110 kDa protein with ten transmembrane segments and contains the binding sites for sodium, potassium, ATP, and cardiac glycosides. In contrast, the β subunit is a smaller, glycosylated, single transmembrane spanning protein with a mass of ~35-60 kDa. Although β subunits do not possess cation translocation sites, they have been shown to modulate the apparent affinity of sodium and potassium ions (Eakle et al., 1994; Hasler et al., 1998), and are important for pump assembly and plasma membrane insertion (Geering et al., 1989; Noguchi et al., 1990). Without β, α subunits are retained in the endoplasmic reticulum (ER) (Laughery et al., 2003).

Another single transmembrane domain subunit, γ, modulates Na^+, K^+-ATPase activity but is not required for essential pump function. This subunit has a molecular weight close to ~10 kDa and is predominantly expressed in the kidney of most animals, though moderate expression has been reported in the brain and eyes at tadpole stages in *X. laevis* (Eid and Brändli, 2001). The expression of γ is not crucial for stable α-β formation, nor necessary for α-β transport out of the ER, but has been shown to modulate pump kinetics by stabilizing the E_1 pump conformation, causing an increase in apparent ATP affinity, and by altering cation affinities at the cytoplasmic sodium activation sites (Béguin et al., 1997; Pu et al., 2002; Therien et al., 1997). Currently two γ splice variants have been described in mammals and each splice variant can be altered through post-translational modifications (Arystarkhova and Sweadner, 2005). However, since the γ subunit, also called FXYD2, is not necessary

for pump assembly and is now classified as a member of the FXYD protein family of Na^+, K^+-ATPase regulators, only the structurally indispensable α and β subunits will be considered here.

Na^+, K^+-ATPase subunit expression

Temporal expression of α and β subunit isoforms occurs in many tissues and has been characterized in a variety of systems during development. In embryonic mice, α3 levels are initially absent from the heart at embryonic day (E) 9.5, but increase steadily between E10.5-E16.5. By postnatal day 4, α3 is clearly expressed in ventricular cardiomyocytes (Herrera et al., 1994). In contrast, analysis of pump subunits in fetal rat whole lung shows that α1 and β1 transcripts increase dramatically between E17 and E20, reaching a maximum just prior to birth before both decreasing at postnatal stages to the low levels seen in adult whole lung (O'Brodovich et al., 1993).

Multiple α and β isoforms are present in fish and murine nervous systems. During zebrafish embryogenesis, a full repertoire of subunit isoforms is expressed. Paralogs of α1, α3, β1, β2, and β3 have all been found in either the brain and/or spinal cord and differential expression exists for each gene (Canfield et al., 2002). In mammals, the predominant neuronal subunits are α3 and β1, while α2, β2, and β3 are found primarily in glial cells (Martín-Vasallo et al., 2000; Watts et al., 1991). The α1 subunit is expressed throughout the central nervous system (Watts et al., 1991). These neural sodium pump isoforms are also developmentally regulated. In rat brain all the

α subunits steadily increase between fetal and neonatal stages, reach their peak at the juvenile stage, and no longer increase later in development (Orlowski and Lingrel, 1988). In contrast, the expression of β1 continues to increase during the first few days following birth, while β2 expression gradually decreases in neurons until it is no longer detectable at adult stages; high expression of β2 is still detected in glial cells (Lecuona et al., 1996).

The Na^+, K^+-ATPase in embryonic *X. laevis* is composed of α1, β1, β2, and β3 subunits (Davies et al., 1996; Eid and Brändli, 2001; Good et al., 1990; Messenger and Warner, 2000). While the α1 subunit is present in a variety of structures including neural plate cells (Davies et al., 1996), only β3 of the known β isoforms has been shown to be expressed in the developing spinal cord (Eid and Brändli, 2001). Temporal regulation of the β3 subunit also occurs during early development, suggesting a possible role for this subunit in neuronal differentiation. β3 mRNA transcript levels initially increase during early neural plate stages (Good et al., 1990). Levels of these transcripts then fall transiently prior to neural tube closure before again increasing expression at early tailbud stages to achieve levels comparable to those prior to downregulation (Messenger and Warner, 2000).

Xenopus laevis* vs. *Xenopus tropicalis

X. laevis is a popular model organism for developmental studies due to several factors. These include the ability to induce females to ovulate by simple hormone injections, the large number of eggs that can be generated per spawning, the relatively

large size of embryos, the ease of embryo manipulation, and the ability of embryos to develop externally in saline solution (Amaya et al., 1998; Hirsch et al., 2002). Over-expression studies are possible in *X. laevis* since DNA or RNA constructs can easily be microinjected early in development (Sive et al., 2000). Because of this tractability, many seminal discoveries in cell biology and embryology have been made with this frog species.

However, the genetics of *X. laevis* are somewhat cumbersome because it has an allotetraploid genome. Many genes have two paralogs; hence, complications are likely to result from using traditional knockdown approaches. The lengthy generation time also makes this frog less than ideal for genetic studies (Carruthers and Stemple, 2006). In the last decade, research has been increasingly conducted in *X. tropicalis*, the smaller and more genetically amenable diploid cousin of *X. laevis*. The developmental staging for both frogs is similar, although *X. tropicalis* prefers warmer temperatures than *X. laevis* and develops at a slightly faster rate (Hirsch et al., 2002). *X. tropicalis* offers all the advantages of *X. laevis* and appears to be more advantageous as a vertebrate genetic system since the genome of *X. tropicalis* is smaller and its generation time is more rapid, with an average of 4-6 months to adulthood instead of 1-2 years for *X. laevis* (Amaya et al., 1998; Beck and Slack, 2001; Hirsch et al., 2002).

As research shifts from using *X. laevis* to *X. tropicalis*, it is important to verify that biological events observed first in *X. laevis* are also seen in *X. tropicalis*. Many of the tools described for *X. laevis*, such as *in situ* hybridization probes, can be directly

applied to *X. tropicalis* and indeed, many genes show similar tissue distribution between the two species (D'Souza et al., 2002; Fletcher et al., 2004; Khokha et al., 2002). However, differences in the temporal profiles or levels of gene expression may exist due to the accelerated development and smaller size of *X. tropicalis* (Knöchel et al., 2001; Sedohara et al., 2006). Depending on the assay, studies that quantify levels of gene expression may also need to be reexamined because of the allotetraploidy of *X. laevis*.

The present work shows that *X. tropicalis* neurons generate calcium spikes and that the developmental window of increased spike activity is shorter in this frog species than the corresponding period of increased spike activity in *X. laevis*. The regulation of the Na^+, K^+-ATPase β3 subunit during development is also different between *X. tropicalis* and that published for *X. laevis*, but coincides with the temporal profile of spontaneous calcium spike activity, suggesting a developmental role for β3 in triggering the onset of calcium spiking in *X. tropicalis*. Perturbation experiments support this interesting role. Potential regulation of other genes by β3 subunit expression and Na^+, K^+-ATPase activity is also discussed.

Acknowledgement

This chapter is expanded from a section of the preprint of "Chang, L.W. and Spitzer, N.C. Spontaneous calcium spike activity in embryonic spinal neurons is driven by developmental expression of the Na^+, K^+-ATPase β3 subunit (in preparation)".

MATERIALS AND METHODS

Xenopus handling and husbandry

X. laevis females were primed with 50U of human chorionic gonadotropin (hCG) (Sigma, St. Louis, MO) 3-7 days prior to use and boosted with 350-450U 8-12 hr prior to *in vitro* fertilization. Males were sacrificed prior to squeezing. The testes were removed and stored at 4°C in 1x MMR (100 mM NaCl, 2 mM KCl, 1 mM $MgSO_4$, 5 mM HEPES, 0.1 mM EDTA, 2 mM $CaCl_2$, pH adjusted to 7.8 with HCl) supplemented with 20% fetal bovine serum and 0.5 mg/mL gentamicin (Lonza Walkersville, Walkersville, MD). Eggs were gently squeezed out of the female into a 60 mm petri dish containing 1x MMR and the fluid decanted until the remaining solution filled approximately 1/10 of the dish. A portion of the extracted testes was then macerated with forceps and swirled in the dish containing harvested eggs. The dish was subsequently filled with deionized ultra-filtered water (Fisher Scientific, Fair Lawn, NJ). After fertilization, embryos were sorted, rinsed with 0.1x MMR and transferred into new petri dishes containing 0.1x MMR.

X. tropicalis embryos were obtained either by natural mating or *in vitro* fertilization. Females were primed with 20U of hCG 24-48 hr prior to boosting with 200U hCG to induce ovulation, while males were primed with 10U and boosted with 100U hCG. Frogs were then randomly paired and allowed to mate in 4 L tanks of 0.1x MMR. For *in vitro* fertilizations, frogs were first naturally mated to assess the fertilization success rate. Once a successful mating pair was identified, testes were freshly dissected from the male frog, homogenized in 1 mL of 1x MMR, and placed on ice. Eggs were massaged out of the female frog, harvested in a dry 60 mm petri

dish, and soaked in testes homogenate. The dish was swirled and then filled with 0.1x MMR. All embryos were staged according to Nieuwkoop and Faber (1967).

Cell culture

Neuron-enriched cultures were prepared from the posterior neural plate of stage 15 *X. laevis* and *X. tropicalis* embryos by first removing the gut and transferring the presumptive spinal cord into 1 mg/ml collagenase B (Roche, Indianapolis, IN) dissolved in modified Ringer's solution (116 mM NaCl, 0.67 mM KCl, 1.31 mM $MgSO_4$, 2 mM $CaCl_2$, 4.6 mM Tris-base, pH adjusted to 7.8 with HCl). The notochord and myotomes were gently lifted away and the underlying neural tissue dissociated in Ca^{2+}, Mg^{2+}-free media (116 mM NaCl, 0.67 mM KCl, 4.6 mM Tris-base, 0.41 mM EDTA, pH adjusted to 7.8 with HCl) for 45-60 min before being plated into 2 mL of modified Ringer in 35 mm tissue-culture treated petri dishes (Corning, Corning, NY). Each dish contained cells from one embryo and all cultures were grown at room temperature (21-23°C).

***In vitro* calcium imaging and spike analysis**

Cultured cells were loaded with a fluorescent calcium indicator to visualize intracellular calcium at various times during *in vitro* development. Prior to imaging, cells were incubated in modified Ringer's solution containing 1.25 μM Fluo-4 AM (Invitrogen/Molecular Probes, Eugene, OR), 0.01% Pluronic F-127 (Invitrogen/Molecular Probes), and 0.2% DMSO (Sigma) for 50-60 min. Cells were

washed 3x after incubation and imaged in modified Ringer. Fluorescence images were acquired with a Bio-Rad MRC-600 argon laser confocal microscope (Bio-Rad, Hercules, CA) using a 20x water immersion objective at 0.2 Hz for 1 hr and analyzed with NIH Image 1.63 (W. Rasband, NIH, http://rsb.info.nih.gov/nih-image/). Young cultures were imaged at 0.2 Hz for 0.5 hr to minimize photodamage. Neurons were allowed to grow and extend neurites several hours after imaging to assess health and to verify neuronal identity in young cultures. Neurons were recognized by their phase-bright cell bodies and dark neurites with lengths ≥1x the cell body diameter. Calcium spikes were determined by their rise time (within 5 sec to peak) and amplitude (>2 standard deviations from the baseline noise fluorescence). Silent neurons were not included in the analysis.

Embryo dissections for *in vivo* imaging

Stage 15-21 embryos were dissected in wells of Sylgard-coated (Dow Corning Corporation, Midland, MI) petri dishes containing 1 mg/mL collagenase B. Briefly, the gut and epidermis surrounding the presumptive spinal cord were cut away with a thin scalpel (Fine Science Tools, Inc., Foster City, CA), the endodermal yolk layer was removed, and embryos were secured to the Sylgard-lined wells ventral side up with 0.10 mm diameter stainless steel Austerlitz Minutien pins (Fine Science Tools, Inc.). After pinning the embryo, the myotomes and notochord were gently removed with sharp forceps, and the solution was replaced with modified Ringer.

In vivo calcium imaging and spike analysis

Presumptive spinal cords were incubated in modified Ringer's solution containing 5 μM Fluo-4 AM, 0.05% Pluronic F-127, and 1% DMSO for 50-60 min. Preparations were then washed 3x and imaged in modified Ringer. Fluorescence images were acquired with a Leica SP5 confocal microscope (Leica, Nussloch, Germany) and a 40x water immersion objective at 0.2 Hz for 0.5 hr and analyzed with NIH Image. Calcium spikes were determined by their rise time (within 5 sec to peak) and amplitude (>2 standard deviations from the baseline noise fluorescence). Preliminary data obtained from Chung (2007) were reanalyzed and grouped with current data. Spinal cords that did not exhibit activity and neurons that did not spike during the imaging period were excluded from the analysis.

Morpholino design

The splice-blocking Na^+, K^+-ATPase β3 subunit lissaminated antisense morpholino oligonucleotide (β3 MO) (5'-AAATGAATGATCGGCTTTCTCACCC-3') was directed to the first splice donor site of the β3 primary RNA sequence and synthesized by GeneTools, LLC (Philomath, OR). The preliminary genomic sequence of the β3 subunit was obtained by aligning the β3 mRNA sequence (GenBank Accession: BC062517) to the JGI *X. tropicalis* genome assembly (v4.1) using the BLAST alignment search tool to determine exon-intron boundaries. Splice junctions were confirmed by amplifying intron 1 of the β3 gene with RT-PCR and sequencing the resulting product (Eton Bioscience, Inc., San Diego, CA). Primers used for intron

amplification were located in exon 1, (5'-CAAGGAAGAGAACAAGGGAAGC-3') and exon 2 (5'-GGTATTTGGGGACAGAATCATC-3'). To verify the identity of alternatively spliced transcripts, primers pE1 (5'-AGAACAAGGGAAGCGAGCAG-3'), pI1 (5'-CAAAGCAAAGCAGACAGAGG-3'), and pE3 (5'-AAGCCCAGCAGATTTAGGAG-3') were used. A standard lissaminated control morpholino (CMO) (5'-CCTCTTACCTCAGTTACAATTTATA-3'), which does not target *Xenopus* genes was also synthesized by GeneTools, LLC and used as a negative control.

Blastomere injections

After fertilization, embryos were transferred to a 2% cysteine solution (in 0.1x MMR, pH adjusted to 8.0 with NaOH) to dissolve jelly coats. Embryos were then thoroughly washed with 0.1x MMR and transferred to a 60 mm plastic mesh-lined petri dish containing 6% Ficoll-400 (Sigma) in 0.1x MMR. For imaging and electrophysiology experiments, one blastomere of a two-cell stage embryo was injected with 10-20 ng of β3 MO. For qRT-PCR, embryos were injected at the one-cell stage with 21-26 ng of β3 MO. Embryos were transferred to fresh Ficoll solution in a petri dish coated with 1% (w/v) agarose in 0.1x MMR after injections. Healthy embryos were then sorted, moved to uncoated petri dishes containing 0.1x MMR, and incubated in the dark.

Electrophysiology

Intracellular recordings were made from neurons in the ventral spinal cord using glass micropipettes backfilled with 1 M potassium acetate. Stage 21/22 embryos were dissected in 1 mg/mL collagenase B as for imaging experiments, transferred to a Sylgard-lined recording chamber filled with modified Ringer, and pinned ventral side up at the rostral and caudal ends. Electrode resistances varied between 25-45 MΩ and membrane potentials were measured *in vivo* within 1 hr of dissection using an Axoclamp-2B amplifier (Axon Instruments, Union City, CA) in bridge mode.

RNA isolation and cDNA synthesis

Total RNA was isolated from whole embryos ranging in development from early neurula to tailbud stages using the RNAqueous®-4PCR Kit (Ambion, Austin, TX). The jelly coats and vitelline membrane of each embryo were removed with sharp forceps prior to RNA harvesting. RNA concentration and quality were determined by diluting samples in nuclease-free H_2O (Fisher Scientific) and measuring the absorbance of each sample at 260 nm and 280 nm. 2.5 μg of total RNA was then reverse-transcribed using the SuperScript III First-Strand Synthesis System for RT-PCR (Invitrogen, Carlsbad, CA) with oligo$(DT)_{20}$ primers. Following reverse transcription, the cDNA was diluted with nuclease-free H_2O and stored in aliquots at -20°C.

Quantitative RT-PCR (qRT-PCR)

Selection of primers was performed with Primer3 (http://frodo.wi.mit.edu/cgi-bin/primer3/primer3_www.cgi) and cross dimer formation was checked with NetPrimer (http://www.premierbiosoft.com/netprimer/netprlaunch/netprlaunch.html). All primers were synthesized by Allele Biotech (San Diego, CA) and used at a final concentration of 200 nM each. Na^+, K^+-ATPase subunit primers are listed in Table 2-1 and candidate gene primers are listed in Table 2-2. A total of 10 ng of cDNA template were used per reaction. Complementary DNA diluted from 11 embryos was used for the Na^+, K^+-ATPase subunit assay per stage and a total of n=4 individual runs from separate clutches of embryos were averaged. The candidate gene studies were carried out from diluted cDNA from 5 embryos either treated or untreated with β3 MO per stage. Final results were obtained from grouping data into 3 stage bins (15-20, 21-24, 25-28) and averaging all values for $n \geq 3$ individual runs from separate clutches of embryos. All reactions were run in triplicate on an ABI PRISM® 7900HT Sequence Detection System (Applied Biosystems, Foster City, CA) with default settings for absolute quantitation using a standard curve and *Power* SYBR® Green PCR Master Mix (Applied Biosystems). Data were analyzed using SDS 2.2.1 (Applied Biosystems).

Construction of plasmid DNA standards for qRT-PCR

Regions of each gene examined were amplified by RT-PCR with Platinum® *Taq* DNA Polymerase High Fidelity (Invitrogen) using the same primers used for

qRT-PCR. RT-PCR products were electrophoresed on a 2% (w/v) agarose/tris-acetate-ethylenediaminetetraacetic acid gel, stained with ethidium bromide and purified with the QIAquick Gel Extraction Kit (Qiagen, Valencia, CA). These fragments were subsequently cloned into pCR®2.1-TOPO vectors using the TOPO TA Cloning Kit (Invitrogen) and the resulting plasmids amplified and purified with the HiSpeed Plasmid Midi Kit (Qiagen). DNA concentration was determined by diluting samples in nuclease-free H_2O and measuring the absorbance of each sample at 260 nm. Each plasmid was diluted in triplicate and the optical density readings averaged to determine final DNA concentration. Samples were sequenced by Eton Bioscience, Inc. to verify that correct inserts were cloned, and each unique DNA standard was serially diluted and stored in aliquots at -80°C.

Statistical analysis

Statistical analyses were performed using GraphPad Prism 5 (GraphPad Software, San Diego, CA). Calcium spike and incidence data were analyzed with Kruskal-Wallis non-parametric tests followed by Dunn's post test and Mann-Whitney U tests. All other data were analyzed with two-tailed paired or unpaired t-tests. Data are presented as means ± s.e.m. Results are considered significant when $p<0.05$.

Acknowledgement

This chapter is taken from the preprint of "Chang, L.W. and Spitzer, N.C. Spontaneous calcium spike activity in embryonic spinal neurons is driven by developmental expression of the Na^+, K^+-ATPase β3 subunit (in preparation)".

Table 2-1. Na^+, K^+-ATPase qRT-PCR primer sequences

Subunit	Forward Primer (5'→3')	Reverse Primer (5'→3')	Length	GenBank Accession
α1	GATGACCGCTGGAATAACGA	CAGGGCAGTAGGACAGGAAG	247 bp	BC064884
β3	CGGACTTTGCTCTGGGATAG	GGGTTTCCTTCTGGCTTCA	108 bp	BC062517

Table 2-2. Candidate gene qRT-PCR primer sequences

Gene	Forward Primer (5'→3')	Reverse Primer (5'→3')	Length	GenBank Accession / Ensembl ID
Orai1	CAAAGCCTCAAGCCGAACT	GCAAATAGATGGACAGCAACC	153 bp	ENSXETT00000053436
Notch1	ACTATGGCAACGAGGAGGAG	AAGCACTGGGAGGAGGATTT	214 bp	BC133053
Olig2	TCTTCCTCCACTATGAGCGACT	CATCTGCTTCTTGTCCTTCTTG	156 bp	ENSXETT00000008123
Olig4	GACAGAGAATGCCTCCCAGA	ATCACTTCCCGCAGACCA	151 bp	NM_001045715, CR848409

EXPERIMENTAL RESULTS

Calcium spikes in *Xenopus* embryonic spinal neurons *in vitro*

Previous studies of calcium spike activity focused on embryonic neurons from the *X. laevis* spinal cord. To exploit the more tractable genetics of *X. tropicalis*, it was necessary to determine whether spike activity in *X. tropicalis* is similar to that in *X. laevis*. Spike frequency averages between 1 to 3 spikes hr^{-1} and is highest between 5-10 hr of development in cultured *X. laevis* neurons grown in media containing 10 mM calcium (Gu et al., 1994; Gu and Spitzer, 1995). To determine the firing frequency in *X. tropicalis* spinal neurons, we performed a similar assay *in vitro,* but cultured neurons in 2 mM instead of 10 mM calcium media because neurons grown in media containing this more physiological concentration of extracellular calcium have been demonstrated to spike at higher frequencies (Gorbunova and Spitzer, 2002). Neural ectoderms of *X. tropicalis* embryos were dissociated, plated and allowed to develop between 3-11 hr in culture. Cells were loaded with the fluorescent calcium indicator dye Fluo-4AM and spike activity was assayed by confocal microscopy with image acquisition at 0.2 Hz (Fig. 3-1A). Digitized traces of fluorescence levels in each neuron over time were then analyzed and scored for spikes (Fig. 3-1B).

The average firing frequency of *X. tropicalis* neurons is highest between 3-5 hr of growth *in vitro*. At these times, neurons spike at a rate of 14.4 ± 5.5 hr^{-1} (n=10) (Fig. 3-1C). During 5-7 hr, the frequency of calcium spikes declines to 3.1 ± 1.1 hr^{-1} (n=11) and average spike frequency does not return to the high levels seen between 3-5 hr at later time points (Kruskal-Wallis, $p<0.05$, followed by Dunn's post test, $p<0.05$).

To determine if the frequencies and developmental time course of calcium spike activity in *X. tropicalis* mirrors that found in *X. laevis*, we also analyzed spike activity in *X. laevis* spinal neurons cultured in 2 mM calcium media. Prior to 5 hr of development, the average number of spikes recorded is 4.9 ± 1.7 hr^{-1} (n=15). Between 5-7 hr, calcium spike frequency increases to 14.4 ± 2.4 hr^{-1} and remains high (16.1 ± 4.6 hr^{-1}) through 7-9 hr of development *in vitro* (n≥15) (Fig. 3-1D). After 9 hr, the number of spikes recorded decreases to 5.0 ± 1.0 hr^{-1} (n=22). The mean frequencies seen between 3-5 and 9-11 hr are significantly different from those seen during the 5-9 hr time window (Kruskal-Wallis, $p<0.001$, followed by Dunn's post test, $p<0.01$). These results demonstrate that while the average numbers of spikes recorded per hr in *X. tropicalis* and *X. laevis* neurons are comparable, the period of higher frequency calcium spiking appears earlier in *X. tropicalis* neurons than in *X. laevis* neurons *in vitro*.

Calcium spikes in *Xenopus* embryonic spinal neurons *in vivo*

Neuron-enriched cultures consist of heterogeneous populations of cells from dorsal and ventral regions of the spinal cord. Although neurons located on both surfaces spike *in vivo* in *X. laevis*, those positioned more ventrally have been demonstrated to spike at higher frequencies (Borodinsky et al., 2004; Gu et al., 1994; Root et al., 2008). We hypothesized that the majority of cultured neurons seen firing calcium spikes are ventral neurons. Therefore, we imaged these neurons at various stage intervals chosen to most closely coincide with *in vitro* development in *X.*

tropicalis to determine the window of calcium spike activity *in vivo*. Stages 21-24 coincide with development between 3-5 hr *in vitro* and stages 25-28 coincide with development between 5-9 hr *in vitro*. Since spike analysis of cultured neurons was not possible prior to 3 hr *in vitro*, we also examined calcium spike activity at stages 17-20, which most closely correspond to these early time points.

Between stages 17-20, spinal neurons are rarely active and few spinal cords exhibit spike activity (n=3 out of 13 spinal cords). Nevertheless, active neurons fire calcium spikes at an average rate of 3.0 ± 1.0 hr^{-1} (n=6). The mean spike frequency increases to 9.1 ± 1.5 hr^{-1} between stages 21-24 and falls back down to 3.2 ± 0.4 hr^{-1} between stages 25-28 ($n \geq 30$) (Kruskal-Wallis, $p<0.001$, followed by Dunn's post test, $p<0.05$) (Fig. 3-1E). These findings indicate that in *X. tropicalis*, spike timing *in vivo* matches spike timing *in vitro*. The incidence of spiking seen in *X. tropicalis* spinal neurons as development progresses *in vivo* also parallels the trend seen for spike frequency. Between stages 17-20, the percentage of spiking neurons in active spinal cords is 3.6 ± 1.1%. The incidence subsequently increases to 9.4 ± 2.2% during stages 21-24 and declines to 4.2 ± 1.1% between stages 25-28 (Fig. 3-1F). In *X. laevis*, these observations are not seen. The duration of high calcium spike activity is longer *in vivo* than *in vitro* and incidence and frequency trends across stages are not related (Borodinsky et al., 2004).

Developmental regulation of Na^+, K^+-ATPase subunits

Sodium pump activity is required for neuronal differentiation of *X. laevis* neurons *in vitro* (Messenger and Warner, 1979). While multiple α and β subunits are expressed in the mammalian central nervous system (Orlowski and Lingrel, 1988; Watts et al., 1991), the neural Na^+, K^+-ATPase in embryonic *X. laevis* consists primarily of α1 and β3 subunits (Eid and Brändli, 2001; Good et al., 1990; Messenger and Warner, 2000). Therefore, we assayed α1 and β3 transcript levels with qRT-PCR from the onset of neurulation through the tailbud stages of developing *X. tropicalis* embryos to determine whether developmental changes in Na^+, K^+-ATPase expression could be involved in regulating calcium spike activity. Data were measured as absolute numbers of transcripts per 10 ng of cDNA template.

At stage 13/14, α1 transcripts are initially low and an increase of ~70% occurs by stage 15/16. These transcript levels are then maintained through stage 28 (Fig. 3-2). Similar to α1, β3 levels are also lowest at stage 13/14 and increase approximately 100% by stage 15/16. However, unlike α1, β3 transcripts remain high through stage 19/20, and then decrease at stage 21/22 to levels comparable to those observed at stage 13/14. A slight increase in β3 occurs beginning at stage 23/24 and transcripts are sustained at this level through stage 28 (Fig. 3-2). In general, we find that β3 transcripts are present in higher amounts than α1 transcripts at all stages examined. Similar observations have been made in several developing rat tissues (Orlowski and Lingrel, 1988), rat skeletal muscle (Lavoie et al., 1997), and mammalian kidney cell

lines, and may be attributed to the more rapid degradation rate of the β subunit compared to the α subunit (Lescale-Matys et al., 1993; Mircheff et al., 1992).

Knockdown of β3 subunit expression alters neuronal membrane potential

These results suggest that temporal regulation of β3 transcripts occurs during two distinct periods of development: neurulation and the appearance of calcium spike activity. The upregulation of β3 during neural tube formation seen here corresponds to a previously reported increase in membrane potential of neural plate cells during nervous system development (Blackshaw and Warner, 1976), and the timing of β3 downregulation coincides with the onset of increased calcium spike activity. Could the upregulation and subsequent downregulation of sodium pump activity be necessary for the appearance of these calcium spikes? To address this question, a β3 MO was designed to sit on the first splice junction to generate an aberrant mRNA transcript that retains intron 1 (Fig. 3-3A). The strategy was to decrease the peak of β3 expression seen between stages 15-20, thereby disrupting sodium pump activity. However, we did not seek to completely eliminate β3 levels since previous studies have shown that knocking out various pump subunits during development is lethal (Ikeda et al., 2003; Ikeda et al., 2004; James et al., 1999; Madan et al., 2007; Magyar et al., 1994).

To check the phenotype of transcripts resulting from the β3 MO, multiplex RT-PCR was carried out on cDNA from stage 15/16 control uninjected, control morpholino (CMO) and β3 MO injected embryos using primers designed to exon 1,

intron 1, and exon 3 (Fig. 3-3A). In control and CMO lanes, a single band corresponding to 257 bp was present. This was the expected size of amplified fragments from a correctly spliced β3 transcript. However, in the β3 MO lane, a larger 421 bp product corresponding to a mis-spliced transcript that retained the first intron was also present in addition to the wild-type fragment (Fig. 3-3B). Sequencing the PCR amplicons confirmed the identity of the wild-type band and showed that translation of the mis-spliced β3 product would cause a frameshift mutation that prematurely truncates the protein after translation of the first exon (Fig. 3-3C).

Embryos injected with the β3 MO did not look morphologically different from control or CMO injected embryos at the stages examined. However, β3 MO-treated embryos were unresponsive to touch when poked a glass probe. This paralysis behavior was observed in over 95% of embryos treated with the β3 MO but not apparent in control or CMO-treated embryos (data not shown).

We hypothesized that reducing β3 expression decreases Na^+, K^+-ATPase activity and affects the membrane potential (V_m) in developing neurons. Accordingly, we measured V_m in ventral spinal neurons treated with and without the β3 MO by first injecting the β3 MO into one blastomere of two-cell stage embryos and allowing embryos to develop until the early tailbud stage. The gut was then removed and the ventral spinal cords pinned and exposed after dissecting out the notochord and myotomes (Fig. 3-4A). Intracellular recordings from neurons in current clamp mode were performed on both β3 MO-treated and control sides of each embryo. Experiments were blinded such that the β3 MO-treated or side was not confirmed by

fluorescence microscopy until after measurements were made. Neurons on the control side display an average V_m of -36.5 ± 1.6 mV (Fig. 3-4B). If decreasing β3 levels decreases Na^+, K^+-ATPase activity, neurons on the β3 MO injected side should have more positive resting potentials than neurons on the control side. Indeed, neurons on the injected side have an average V_m of -19.6 ± 1.6 mV, which is significantly different from controls (Two-tailed unpaired t-test, $p<0.0001$) (Fig. 3-4B).

Knockdown of β3 subunit expression reduces calcium spiking

To determine whether Na^+, K^+-ATPase expression plays a role in regulating calcium spike activity, we again injected single blastomeres with the β3 MO at the two-cell stage, allowed embryos to develop, and imaged ventral spinal neurons loaded with Fluo-4AM between stages 17-24 to assay spike frequency and incidence (Fig. 3-5A). The half of the spinal cord treated with β3 MO was identified by red fluorescence (Fig. 3-5B) and the merged image revealed that spiking neurons were predominantly located on the control side (Fig. 3-5C).

Prior to neural tube closure (stages 17-20), the percentage of neurons that spiked on the β3 MO-treated side was 1.2 ± 0.7% while the percentage of spiking neurons on the control side was 3.5 ± 1.4% (n=4 spinal cords) (Fig. 3-5D). These numbers are not statistically significant. However, the difference in the number of spiking cells between treated and untreated halves of each spinal cord is notable during stages 21-24. The incidence of spiking neurons on the control side is 10.3 ± 3.1% at these stages. When β3 is knocked down, the percentage of active neurons

drops to 1.0 ± 0.7% (n=7 spinal cords) (Mann-Whitney U Test, $p<0.05$). The statistically significant change in incidence between β3 MO-treated and untreated embryos during stages 21-24, but not 17-20, indicates that β3 expression is necessary between stages 17-20 for the initiation of calcium spike activity.

Spike frequencies in control and β3 MO-treated neurons also follow similar trends. During stages 17-20 neurons on the β3 MO-treated side of the spinal cord fire spikes at a rate of only 2 hr^{-1}, which does not differ considerably from the control side frequency of 3.0 ± 1.0 hr^{-1}. Between stages 21-24, β3 knockdown reduces the mean spiking rate to 4.0 ± 1.2 hr^{-1}. This is lower than the average spike frequency seen on the control side (10.5 ± 2.1 hr^{-1}), although not statistically different (Fig. 3-5E).

Na^+, K^+-ATPase activity and gene expression

Neuronal calcium signals utilize calcium influx from voltage-gated channels located in the plasma membrane as well as calcium released from intracellular stores located in the ER (Berridge, 1998); both are required to generate calcium spike activity (Gu et al., 1994; Holliday et al., 1991; Holliday and Spitzer, 1990). The mechanisms of calcium release from stores involving activity of inositol triphosphate and ryanodine receptors are well described (Berridge, 1998); the latter appear to mediate calcium-induced calcium release in spiking neurons (Gu et al., 1994; Holliday et al., 1991). In comparison, less is known about the mechanisms of store-operated calcium entry (SOCE) and store-operated channels (SOC), which replenish depleted calcium stores. The most notable SOC is the calcium release-activated calcium

(CRAC) channel. It is now recognized that the tetra-spanning plasma membrane protein CRAC modulator 1 (Orai1) constitutes the pore-forming subunit of the CRAC channel. Orai1 is activated by the calcium sensor stromal interaction molecule 1, which is located in the ER membrane (Lewis, 2007; Soboloff et al., 2006; Vig et al., 2006). Although SOCs and SOCE have been studied mainly in non-excitable cells, evidence now suggests that SOCE is also present in neurons (Bouron, 2000; Emptage et al., 2001; Tobin et al., 2006).

It has recently been shown that *Orai1* may have functions in the developing nervous system (Koizumi et al., 2007). To determine if this gene is also present in *X. tropicalis* and whether knockdown of β3 affects its expression, qRT-PCR was used to evaluate *Orai1* transcript levels in developing embryos between stages 15-28. Data were measured as absolute numbers of transcripts per 10 ng of cDNA template, as for the Na^+, K^+-ATPase subunit analyses, and results were grouped and averaged into stages corresponding to developmentally significant events between stages 15-28: upregulation of β3 expression (stages 15-20), increased calcium spike activity (stages 21-24), and post calcium spike activity (stages 25-28).

In wild-type embryos, *Orai1* transcripts are present throughout stages 15-20 and increase approximately 25% during development between stages 15-20 and 21-24 (Fig. 3-6A). Transcripts then remain at this elevated level through stage 28. When β3 is knocked down, *Orai1* expression decreases concomitantly. At stages 15-20 and 21-24, transcript levels fall 25% and 35%, respectively from levels seen in wild-type embryos. *Orai1* transcripts then increase slightly from stages 21-24 to stages 25-28,

although levels are still significantly lower than those seen in wild-type embryos (Two-tailed paired t-test, $p<0.05$).

To determine whether modulation of Na^+, K^+-ATPase activity affects expression of other genes, transcript levels of *Notch homolog 1* (*Notch1*), *oligodendrocyte transcription factor 2* (*Olig2*) and *oligodendrocyte transcription factor 4* (*Olig4*) in treated and untreated embryos were also examined. These genes were chosen as controls for the β3 MO treatment. Notch signaling plays roles in cell-fate determination including the maintenance of neuronal progenitors and neuronal and glial differentiation (Louvi and Artavanis-Tsakonas, 2006; Shimojo et al., 2008), while the *olig* genes are basic helix-loop-helix transcription factors thought to be important for oligodendrocyte development. *Olig2* is located on the ventral surface of the spinal cord and is required for maintaining motoneuron and oligodendrocyte precursors (Kessaris et al., 2001; Lu et al., 2002; Rowitch, 2004; Zhou and Anderson, 2002; Zhou et al., 2001). The less well characterized *Olig4* is localized to the dorsal spinal cord and to date has only been found in the genomes of fish and amphibians (Bronchain et al., 2007). Nonetheless, its expression seems to be necessary for the differentiation of interneurons and astrocytes (Bronchain et al., 2007; Filippi et al., 2005).

A slight drop in the number of *Notch1* transcripts occurs between stages 21-24 in wild-type embryos. However, this is not significantly different from the levels seen at stages 15-20 or stages 25-28. Similarly, no noticeable increase or decrease in transcripts was apparent between stages 15-28 among wild-type and β3 MO-treated

embryos (Fig. 3-6B). The difference in *olig* gene expression among wild-type and β3 MO-treated embryos was also insignificant. *Olig2* transcripts remain stable throughout the stages examined and *Olig4* levels steadily decrease during development (Fig. 3-6C-D). Thus, while *Orai1* expression is markedly decreased by changes in β3 expression, *Notch1*, *Olig2*, and *Olig4* expression are not affected by β3 knockdown.

Acknowledgement

This chapter is taken from the preprint of "Chang, L.W. and Spitzer, N.C. Spontaneous calcium spike activity in embryonic spinal neurons is driven by developmental expression of the Na^+, K^+-ATPase β3 subunit (in preparation)".

Figure 3-1. Embryonic amphibian spinal neurons exhibit Ca^{2+} spike activity during growth *in vitro* and *in vivo*. (**A-B**) Imaging Ca^{2+} spikes *in vitro*. (**A**) Cells cultured from a dissected stage 15 neural plate of a *X. tropicalis* embryo loaded with Fluo-4AM. Arrows identify cells generating spontaneous spikes during a 1 hr imaging period at 3 hr in culture, prior to neurite outgrowth. Scale bar is 50 μm. (**B**) Ca^{2+} spike activity from the neuron indicated by a large arrow in **A**. (**C-D**) Distinct periods of increased spike activity occur during neuronal development in two different frog species. Values are presented as means ± s.e.m. for n=9-23 neurons/group (**p<0.01, *p<0.05). (**C**) In *X. tropicalis* neurons, Ca^{2+} spike frequency is highest between 3-5 hr of development. (**D**) Ca^{2+} spike frequency of *X. laevis* neurons is highest between 5-9 hr of development. (**E-F**) Ca^{2+} spike activity is elevated in *X. tropicalis* neurons *in vivo* at the corresponding time of development *in vitro*. Values are means ± s.e.m. for n=3-10 embryos/stage. (**E**) Neurons on the ventral surface of the spinal cord exhibit high frequencies of Ca^{2+} spiking between stages 21-24 (**p<0.01, *p<0.05). (**F**) The incidence of spiking on the ventral spinal cord is also high at these stages.

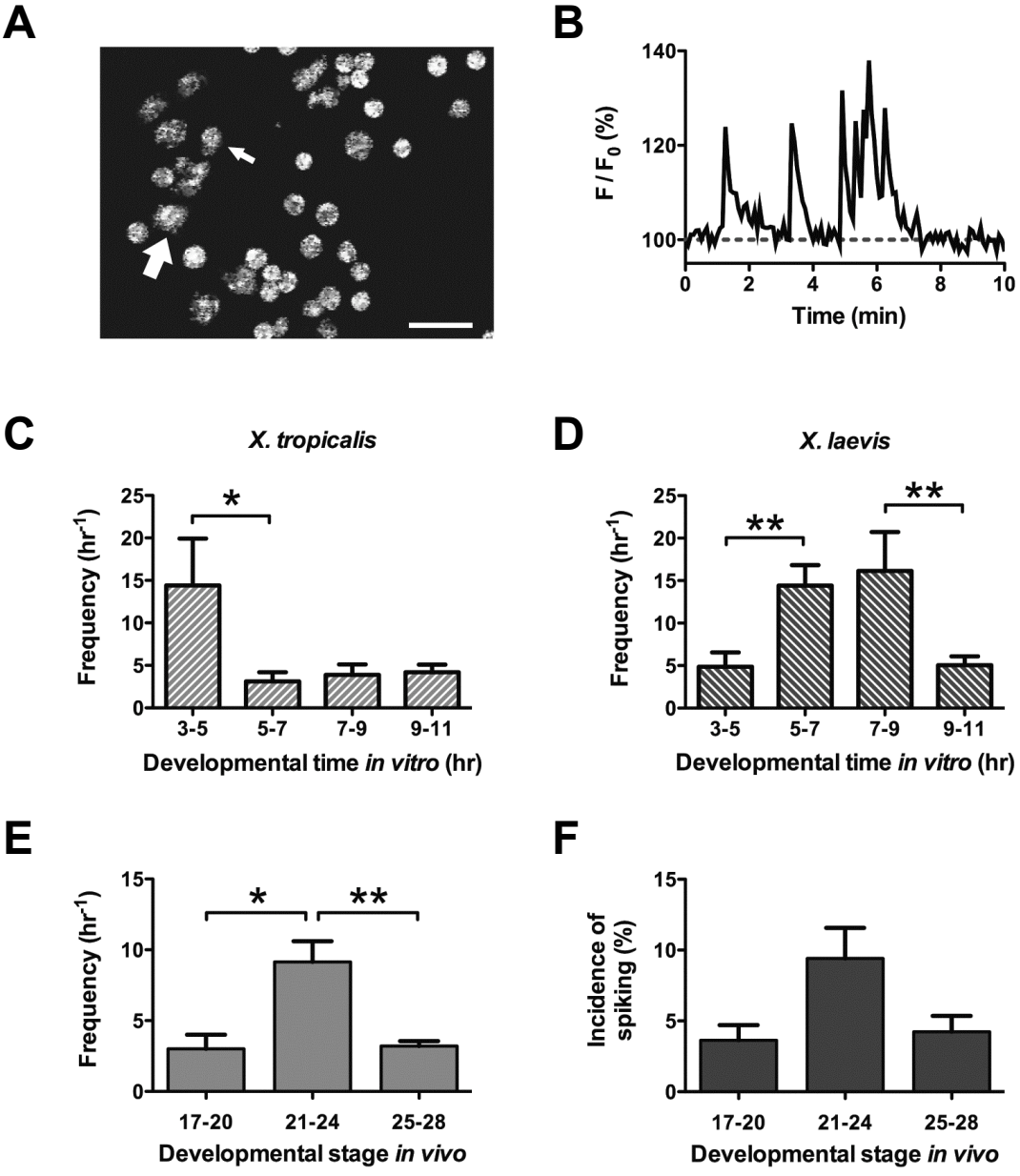
A
B
140
120
100
F / F0 (%)
0
2
4
6
8
10
Time (min)
C
X. tropicalis
Frequency (hr-1)
25
20
15
10
5
0
*
3-5
5-7
7-9
9-11
Developmental time in vitro (hr)
D
X. laevis
Frequency (hr-1)
**
**
3-5
5-7
7-9
9-11
Developmental time in vitro (hr)
E
Frequency (hr-1)
15
10
5
0
*
**
17-20
21-24
25-28
Developmental stage in vivo
F
Incidence of spiking (%)
15
10
5
0
17-20
21-24
25-28
Developmental stage in vivo

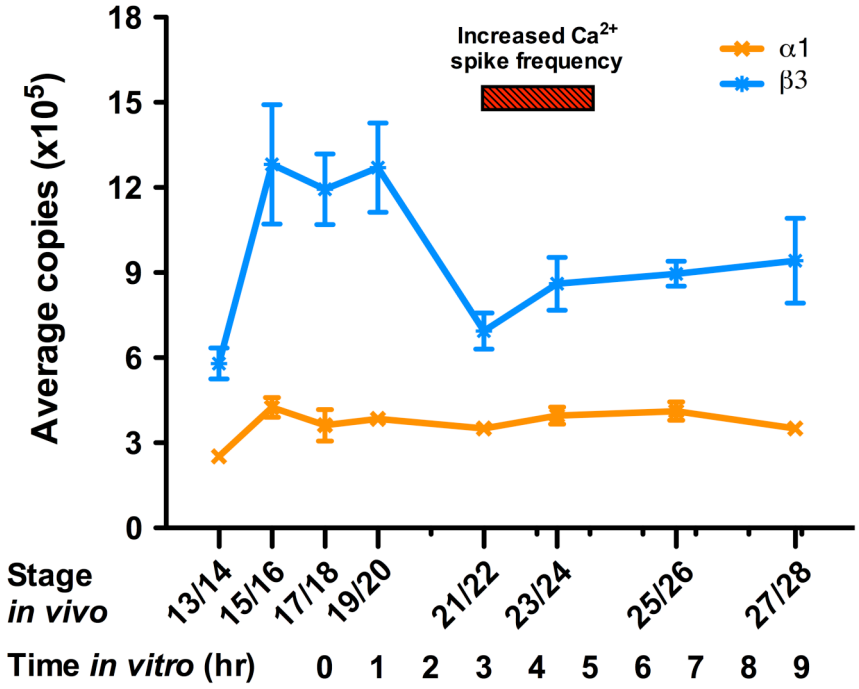

Figure 3-2. Temporal expression of Na^+, K^+-ATPase α1 and β3 subunits in *X. tropicalis* embryos during development. Quantitative RT-PCR shows that β3 mRNA transcript levels are upregulated during development between stages 15-20, while no significant fluctuation of α1 mRNA transcript levels occurs between stages 15-28. β3 transcript levels are downregulated at stage 21/22, coinciding with the period of increased Ca^{2+} spiking observed both *in vivo* and *in vitro*. Values are means ± s.e.m. for n=4 independent experiments.

Figure 3-3. A splice-blocking β3 MO disrupts normal splicing in *X. tropicalis* and predicts translation of a truncated protein in addition to wild-type protein. (**A**) Schematic of β3 un-spliced RNA and the β3 MO target sequence. (**B**) RT-PCR of stage 15/16 β3 MO injected embryos using primers pE1, pE3, and pI1, which flank intron I1 and the exon E1-intron I1 splice junction, amplifies an alternatively spliced 421 bp fragment in addition to the expected wild-type 257 bp fragment. Control uninjected and CMO-treated embryos do not produce alternatively spliced β3 mRNA. (**C**) Spliced β3 mRNA resulting from β3 MO treatment. Conceptual translation of wild-type β3 mRNA produces a 279 amino acid protein (top) while conceptual translation of alternatively spliced β3 mRNA produces a 54 amino acid protein (bottom). The last 18 amino acids of this truncated protein, shown in red, are translated from I1. Asterisks represent the stop codon location in each transcript.

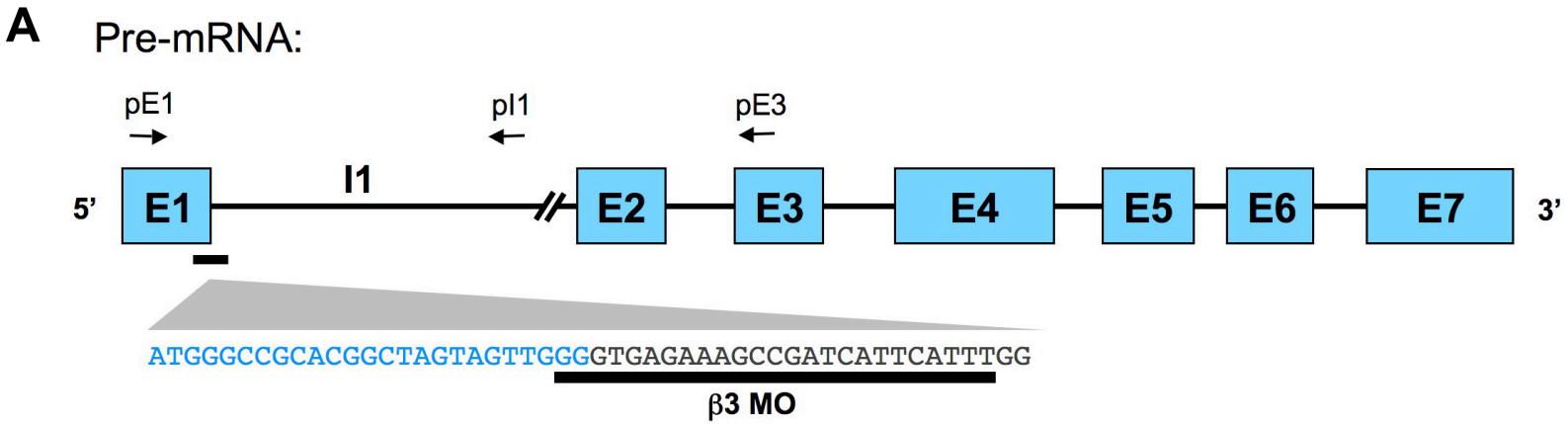
A
Pre-mRNA:
pE1
pI1
pE3
5'
E1
I1
E2
E3
E4
E5
E6
E7
3'
ATGGGCCGCACGGCTAGTAGTTGGGGTGAGAAAGCCGATCATTCATTTGG
β3 MO

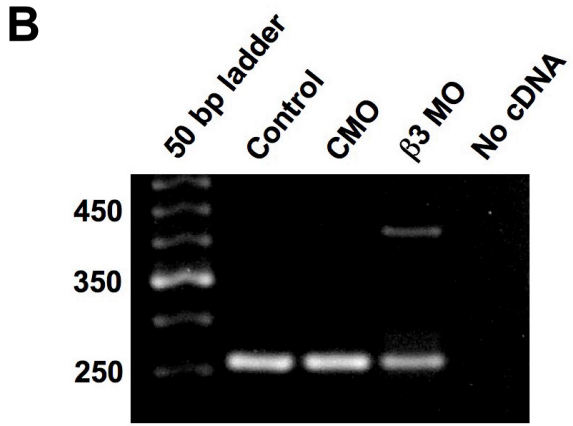
B
50 bp ladder
Control
CMO
β3 MO
No cDNA
450
350
250

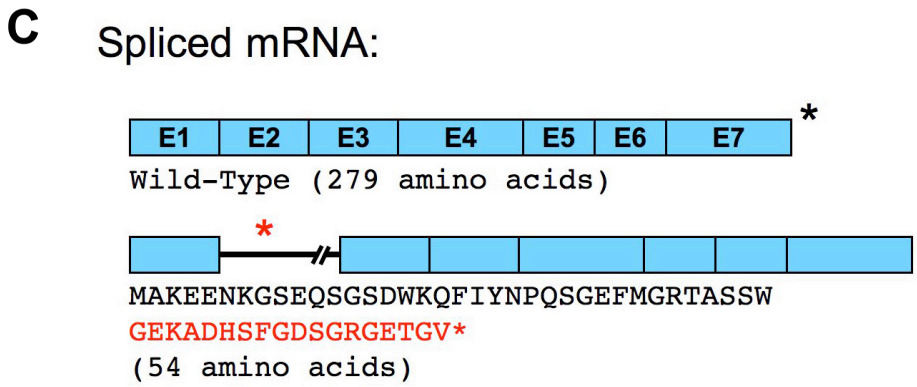
C
Spliced mRNA:
E1
E2
E3
E4
E5
E6
E7
*
Wild-Type (279 amino acids)
*
MAKEENKGSEQSGSDWKQFIYNPQSGEFMGRTASSW
GEKADHSFGDSGRGETGV*
(54 amino acids)

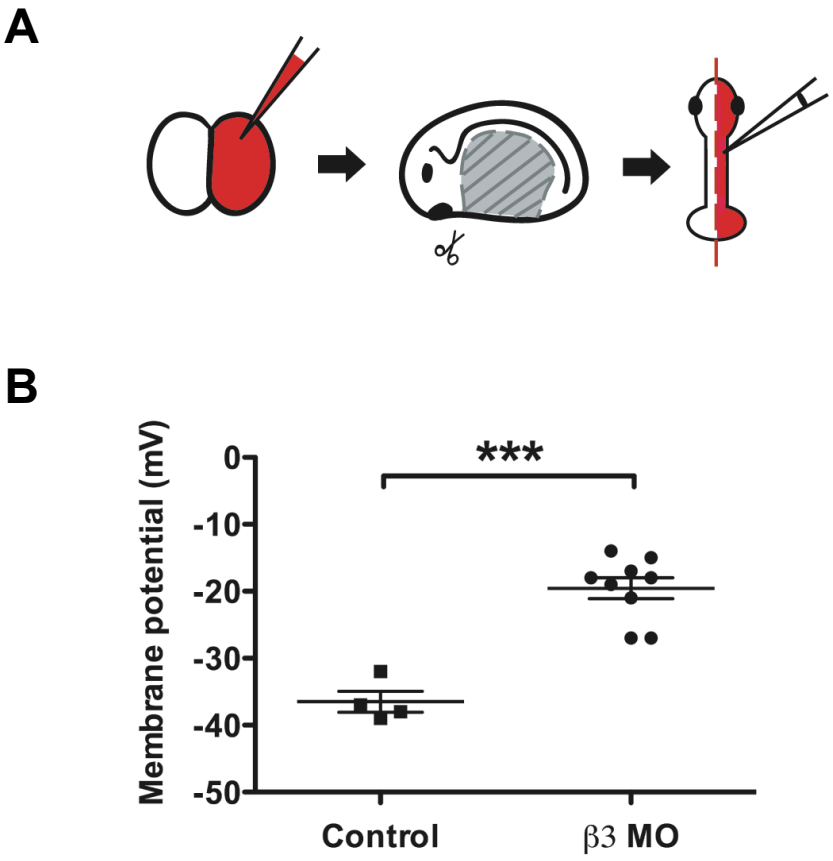

Figure 3-4. The membrane potential of embryonic spinal neurons is depolarized by β3 knockdown. (**A**) At the two-cell stage, a single blastomere is injected with lissamine-tagged β3 MO and the embryo is allowed to develop until stage 21/22. After dissection, intracellular recordings are performed on neurons from β3 MO-treated and untreated sides of the ventral spinal cord. (**B**) Neurons treated with β3 MO display significantly more positive membrane potentials than neurons on the control side (***$p<0.0001$). Each point represents a recording from a single neuron. Horizontal lines represent the mean ± s.e.m.

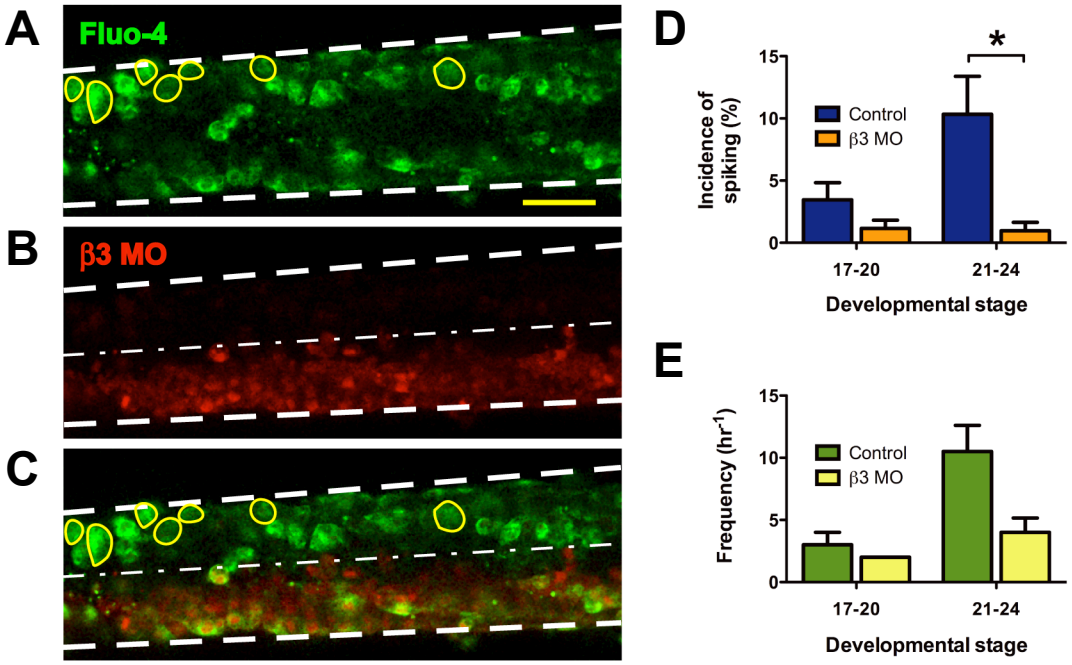

Figure 3-5. Ca^{2+} imaging of ventral spinal neurons from β3 MO-treated embryos. (**A**) A spinal cord is shown loaded with Fluo-4AM in green. Spiking neurons are outlined in yellow; the margins of the spinal cord are indicated by bold dashed lines. Scale bar is 50 μm. (**B**) The half of the spinal cord treated with β3 MO is labeled in red. The thin dashed line indicates the midline. (**C**) A merged image of **A** and **B** shows that spiking neurons are more prevalent on the control side of the embryo. (**D**) The incidence of spiking neurons is significantly reduced in β3 MO-treated neurons compared to controls between stages 21-24 but not different between stages 17-20 (*$p<0.05$). (**E**) β3 knockdown does not affect the frequency of spikes observed at stages 17-20. Between stages 21-24, frequency appears reduced from control levels. Values are means ± s.e.m. for n=4-7 embryos/stage.

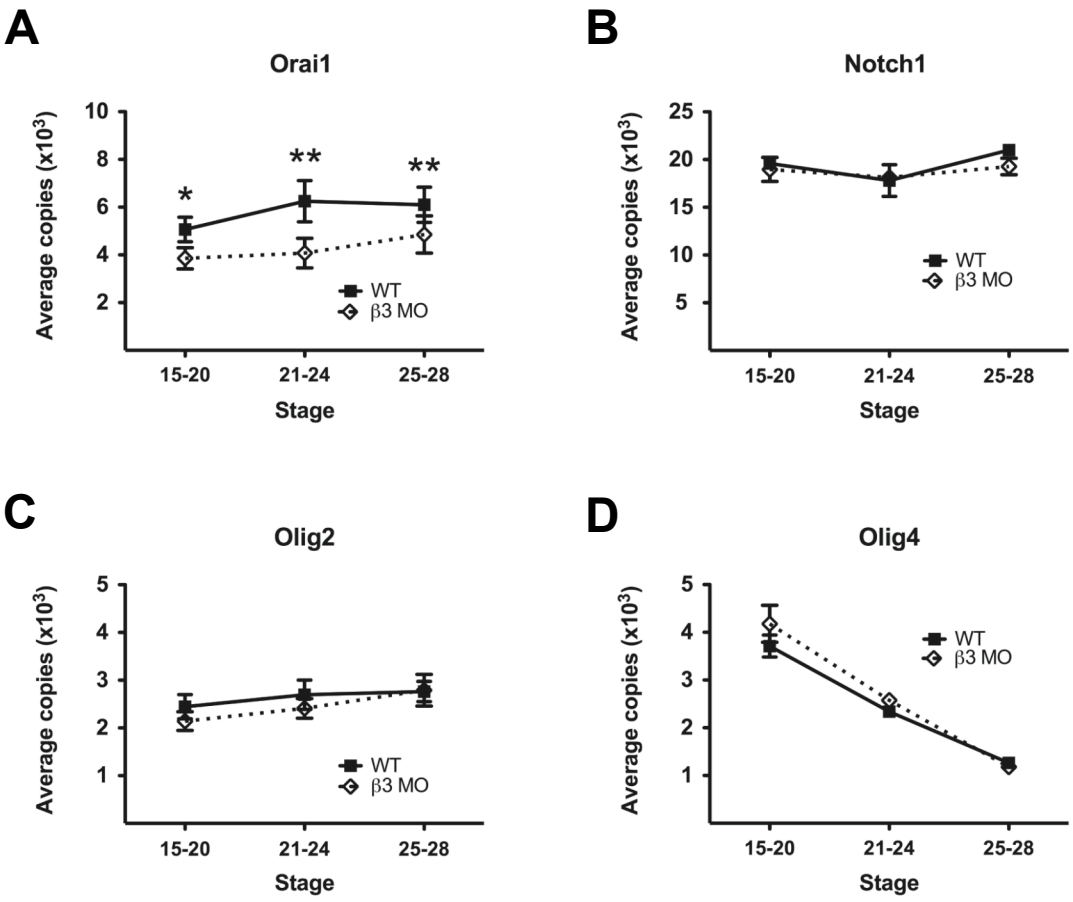

Figure 3-6. Decreased sodium pump activity reduces Orai1 gene expression during embryonic development. (**A**) When β3 levels are lowered, transcript levels of Orai1 are significantly reduced between stages 15-28. Decreased β3 levels do not cause significant changes in (**B**) Notch1, (**C**) Olig2, and (**D**) Olig4 transcripts at the stages examined. All values are means ± s.e.m. for n≥3 independent experiments (**p<0.01, *p<0.05).

DISCUSSION

Determining the regulation of sodium pump activity during early neuronal development is critical to understanding the mechanisms that drive spontaneous calcium spiking. The Na^+, K^+-ATPase directly affects the ionic gradients necessary to maintain membrane potentials, which in turn, influence activation of voltage-gated channels. During embryonic development of *X. tropicalis*, neuronal calcium spikes occur within a window of development after neural tube closure but prior to the formation of fully functional synapses. Expression of the Na^+, K^+-ATPase β3 subunit is upregulated during neurulation and downregulated by the time calcium spikes appear. Blocking this temporal upregulation shifts membrane potentials to more depolarized values and inhibits the appearance of spontaneous calcium spikes. These results support a model that requires activation of the Na^+, K^+-ATPase to initiate the cascade of events necessary for spike production (Fig. 4-1).

β3 regulation and calcium channel activity

Developmental β3 expression is required for the appearance of calcium spikes during neuronal development, linking Na^+, K^+-ATPase activity with calcium signaling. However, the mechanism by which increased β3 expression leads to activation of calcium channels necessary for spike production remains speculative. We suggest that blocking Na^+, K^+-ATPase activity prior to neural tube formation may reduce channel insertion into the membrane or prevent activation of LVA calcium currents.

LVA T-type calcium currents appear early in neuronal development prior to HVA N- and L-type calcium currents in several neuronal populations, including mammalian hippocampal neurons (Yaari et al., 1987), chick sensory dorsal root ganglia (Gottmann et al., 1988), and chick motoneurons (McCobb et al., 1989). These LVA currents are activated at much lower thresholds than HVA currents and are present in embryonic *X. laevis* spinal neurons (Desarmenien et al., 1993; Gu and Spitzer, 1993). The importance of LVA current for calcium spike activity has been demonstrated in cultured neurons. Blocking this current eliminates calcium spike activity as effectively as inhibiting HVA current, indicating a role for LVA current in activating HVA currents (Gu and Spitzer, 1993).

The average membrane potential obtained when β3 expression levels are decreased is notably more positive than the half-activation voltage of neuronal T current in cultured *X. laevis* spinal neurons (Gu and Spitzer, 1993), suggesting that the failure of spike generation could be due to inhibition of LVA current activation. This would then prevent HVA activation and calcium-induced calcium release. It is also possible that failure to activate LVA current prevents HVA channel expression. Blocking T-type calcium channel activity early in development inhibits subsequent HVA calcium channel expression in NG108-15 neuroblastoma-glioma cells that are able to recapitulate well-characterized neuronal properties (Chemin et al., 2002). However, whether this occurs in *Xenopus* spinal neurons has yet to be determined.

In addition, we find that knocking down β3 expression also decreases the transcription of *Orai1*, which encodes a pore-forming subunit of a store-operated

calcium channel, suggesting that there may be a decline in the number of SOCs present in the plasma membrane, leading to a reduction in store refilling. Since calcium spikes depend on calcium-induced calcium release, the suppression of spike activity under these conditions is consistent with decreased *Orai1* transcript levels.

β3 regulation and neuronal differentiation

Differentiation of embryonic cultured *X. laevis* neurons is inhibited when sodium pump activity is blocked during neurulation by strophanthidin, a cardiac glycoside that reversibly binds to the Na^+, K^+-ATPase (Messenger and Warner, 1979). To determine if the lack of calcium spike activity, a corollary of untimely β3 downregulation, could be attributed to failure of neurons to differentiate from precursors or the respecification of neurons to other cell types, we examined the expression levels of three genes involved in regulating neuronal and glial differentiation following β3 knockdown: *Notch1*, *Olig2*, and *Olig4*. However, no significant changes in any of these transcripts were observed. It is possible that gene expression profiles may change outside the developmental period examined. Likewise, changes in expression of other ligands or transcription factors, such as *Delta* or the neurogenin genes, which are needed to interact with these candidate molecules in order to regulate differentiation, may also have ensued following the alteration of β3 expression. Because transcripts of those genes were not analyzed, conclusions regarding cell fate choices in β3 knockdown embryos cannot be drawn.

Downregulation of *Notch* transcripts has been reported following inhibition of pump activity during neurulation with the cardiac glycoside strophanthidin (Messenger and Warner, 2000). This may have resulted either from species variation or from the severity of the knockdown strategy employed. The morpholino concentrations used here likely inhibit pump activity to a lesser extent and cause fewer overtly abnormal phenotypes than the strophanthidin concentrations used by Messenger and Warner (2000), raising the possibility that the β3 MO treatment may be ineffective at reducing Na^+, K^+-ATPase expression. However, this seems doubtful for two reasons. When β3 levels are reduced, the membrane potential of ventral neurons becomes more depolarized compared to control neurons, consistent with reduced Na^+, K^+-ATPase activity. Moreover, the paralyzed phenotype seen with the β3 knockdown embryos is also observed in animals with abnormal α subunit expression in other systems. Newborn mice lacking the α2 isoform exhibit no motor activity and die shortly after birth from lack of respiratory activity even though they have beating hearts (Moseley et al., 2003), while a mutation in the sole *Drosophila* α subunit causes bang-sensitive paralysis that is phenocopied in wild-type flies injected with ouabain (Schubiger et al., 1994).

Other modes of calcium spike regulation

Recent work has shown that GABA and glutamate can bind to metabotropic receptors and regulate calcium spike activity in *X. laevis*. When these receptors are blocked, the incidence of spiking neurons decreases, supporting a model in which

neurotransmitters modulate spike activity (Root et al., 2008). In contrast, our present findings support a model that utilizes an intrinsically encoded mechanism for regulating the onset of calcium spike activity. It was suggested that different neuronal populations may employ different mechanisms for generating calcium spike activity, since blocking these receptors with pharmacological antagonists only prevents a subpopulation of neurons from spiking (Root et al., 2008). Neurons may take advantage of different machinery for initiating the period of calcium spiking in different species as well. It would be interesting to determine whether reducing sodium pump activity alters GABA and glutamate expression in the developing spinal cord prior to the onset of activity and whether the two separate models converge. Reducing sodium pump activity during early neuronal development could first prevent calcium channel activation or insertion, which would then preclude effects of neurotransmitter receptor activation on calcium spike activity. Alternatively, the intracellular signaling cascades activated by these metabotropic receptors may impact Na^+, K^+-ATPase function and provide a feedback mechanism, with which to regulate calcium spiking. Answers to these questions will further elucidate mechanisms by which electrical activity is regulated in young neurons.

Potential mechanisms terminating calcium spike activity

We propose that developmental expression of the Na^+, K^+-ATPase during development is necessary to drive the onset of calcium spike activity, but it is unknown whether the pump plays a role in terminating the period of calcium spiking.

Later upregulation of the pump could, in theory, hyperpolarize neurons and consequently shut down spike machinery. A moderate increase in β3 expression is observed at later stages, which coincides with the termination of spike activity. However, this rise in β3 alone seems insufficient to account for the disappearance of spikes. Increased expression of outward potassium currents contributes to the termination of calcium-dependent action potentials (Lockery and Spitzer, 1992; O'Dowd et al., 1988), indicating that developmental expression of potassium channels or the developmental rates of channel activation may play an important role in ending spike activity. It would be of interest to make electrophysiological recordings of calcium and potassium currents at these stages to determine whether changes in channel activity are a consequence of altered β3 expression.

Additional roles for β3

Are there additional roles for the Na^+, K^+-ATPase β3 subunit in addition to facilitating ion transport? In murine systems the Na^+, K^+-ATPase β2 subunit functions as an adhesion molecule on glia, which is involved in neuron-astrocyte adhesion and promotes neurite outgrowth in a calcium-independent manner (Antonicek et al., 1987; Gloor et al., 1990; Müller-Husmann et al., 1993). Interestingly, more recent work also demonstrates that β1 has roles in cell-cell adhesion (Shoshani et al., 2005; Vagin et al., 2006) and the formation of trophectoderm tight junctions (Madan et al., 2007). This adhesion role appears to be shared among β subunit isoforms of voltage-gated sodium channels as well; the β2 subunit binds to the extracellular matrix molecules tenascin-C

and tenascin-R, and the β1 subunit can bind to the cell-adhesion molecules Nf186, contactin, and NrCAM (McEwen and Isom, 2004; Srinivasan et al., 1998). While no studies to date show that the β3 subunit of the Na^+, K^+-ATPase has adhesion functions, it would nevertheless be interesting to look into whether altering β3 expression affects cellular processes such as neuronal migration and neurite outgrowth during development.

Acknowledgement

This chapter is taken from the preprint of "Chang, L.W. and Spitzer, N.C. Spontaneous calcium spike activity in embryonic spinal neurons is driven by developmental expression of the Na^+, K^+-ATPase β3 subunit (in preparation)".

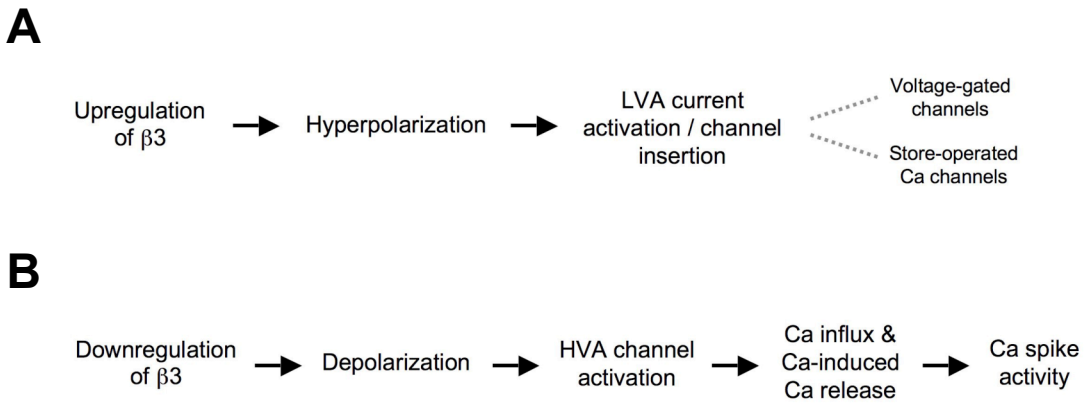

Figure 4-1. Model of the roles of β3 expression during neuronal development. (**A**) Upregulation of β3 hyperpolarizes neurons, allowing activation of low voltage-activated (LVA) calcium current and/or insertion of voltage-gated or store-operated channels. (**B**) Subsequent downregulation of β3 triggers a cascade of events necessary for Ca^{2+} spike production.

REFERENCES

Amaya, E., Offield, M.F., and Grainger, R.M. (1998). Frogs genetics: *Xenopus tropicalis* jumps into the future. Trends Genet. *14*, 253-255.

Antonicek, H., Persohn, E., and Schachner, M. (1987). Biochemical and functional characterization of a novel neuron-glia adhesion molecule that is involved in neuronal migration. J. Cell Biol. *104*, 1587-1595.

Arystarkhova, E., and Sweadner, K.J. (2005). Splice variants of the gamma subunit (FXYD2) and their significance in regulation of the Na,K-ATPase in kidney. J. Bioenerg. Biomembr. *37*, 381-386.

Beck, C.W., and Slack, J.M. (2001). An amphibian with ambition: a new role for *Xenopus* in the 21st century. Genome Biol. *2*, REVIEWS1029.

Béguin, P., Wang, X., Firsov, D., Puoti, A., Claeys, D., Horisberger, J.-D., and Geering, K. (1997). The γ subunit is a specific component of the Na,K-ATPase and modulates its transport function. EMBO J. *16*, 4250-4260.

Berridge, M.J. (1998). Neuronal calcium signalling. Neuron *21*, 13-26.

Blackshaw, S.E., and Warner, A.E. (1976). Alterations in resting membrane properties during neural plate stages of development of the nervous system. J. Physiol. *255*, 231-247.

Blanco, G., Koster, J.C., and Mercer, R.W. (1994). The α subunit of the Na,K-ATPase specifically and stably associates into oligomers. Proc. Natl. Acad. Sci. USA *91*, 8542-8546.

Borodinsky, L.N., Root, C.M., Cronin, J.A., Sann, S.B., Gu, X., and Spitzer, N.C. (2004). Activity-dependent homeostatic specification of transmitter expression in embryonic neurons. Nature *429*, 523-530.

Bouron, A. (2000). Activation of a capacitative Ca^{2+} entry pathway by store depletion in cultured hippocampal neurones. FEBS Lett. *470*, 269-272.

Bronchain, O.J., Pollet, N., Ymlahi-Ouazzani, Q., Dhorne-Pollet, S., Helbling, J.C., Lecarpentier, J.E., Percheron, K., and Wegnez, M. (2007). The *olig* family: phylogenetic analysis and early gene expression in *Xenopus tropicalis*. Dev. Genes Evol. *217*, 485-497.

Brosenitsch, T.A., and Katz, D.M. (2001). Physiological patterns of electrical stimulation can induce neuronal gene expression by activating N-type calcium channels. J. Neurosci. *21*, 2571-2579.

Canfield, V.A., Loppin, B., Thisse, B., Thisse, C., Postlethwait, J.H., Mohideen, M.-A.P.K., Rajarao, S.J.R., and Levenson, R. (2002). Na,K-ATPase α and β subunit genes

exhibit unique expression patterns during zebrafish embryogenesis. Mech. Dev. *116*, 51-59.

Carruthers, S., and Stemple, D.L. (2006). Genetic and genomic prospects for *Xenopus tropicalis* research. Semin. Cell Dev. Biol. *17*, 146-153.

Chemin, J., Nargeot, J., and Lory, P. (2002). Neuronal T-type α1H calcium channels induce neuritogenesis and expression of high-voltage-activated calcium channels in the NG108-15 cell line. J. Neurosci. *22*, 6856-6862.

Chung, S. (2007). Spontaneous calcium spike activity of embryonic neurons of *Xenopus tropicalis*. M.S. thesis in Biological Sciences (University of California, San Diego, La Jolla).

Conklin, M.W., Lin, M.S., and Spitzer, N.C. (2005). Local calcium transients contribute to disappearance of pFAK, focal complex removal and deadhesion of neuronal growth cones and fibroblasts. Dev. Biol. *287*, 201-212.

Créton, R., Kreiling, J.A., and Jaffe, L.F. (2000). Presence and roles of calcium gradients along the dorsal-ventral axis in Drosophila embryos. Dev. Biol. *217*, 375-385.

D'Souza, A., Lee, M., Taverner, N., Mason, J., Carruthers, S., Smith, J.C., Amaya, E., and Zorn, A.M. (2002). Molecular components of the endoderm specification pathway in *Xenopus tropicalis*. Dev. Dyn. *226*, 118-127.

Davies, C.S., Messenger, N.J., Craig, R., and Warner, A.E. (1996). Primary sequence and developmental expression pattern of mRNAs and protein for an α1 subunit of the sodium pump cloned from the neural plate of *Xenopus laevis*. Dev. Biol. *174*, 431-447.

Desarmenien, M.G., Clendening, B., and Spitzer, N.C. (1993). *In vivo* development of voltage-dependent ionic currents in embryonic *Xenopus* spinal neurons. J. Neurosci. *13*, 2575-2581.

Donnet, C., Arystarkhova, E., and Sweadner, K.J. (2001). Thermal denaturation of the Na,K-ATPase provides evidence for α-α oligomeric interaction and γ subunit association with the C-terminal domain. J. Biol. Chem. *276*, 7357-7365.

Eakle, K.A., Kabalin, M.A., Wang, S.-G., and Farley, R.A. (1994). The influence of β subunit structure on the stability of Na^+/K^+-ATPase complexes and interaction with K^+. J. Biol. Chem. *269*, 6550-6557.

Eid, S.R., and Brändli, A.W. (2001). *Xenopus* Na,K-ATPase: primary sequence of the β2 subunit and *in situ* localization of α1, β1, and γ expression during pronephric kidney development. Differentiation *68*, 115-125.

Emptage, N.J., Reid, C.A., and Fine, A. (2001). Calcium stores in hippocampal synaptic boutons mediate short-term plasticity, store-operated Ca^{2+} entry, and spontaneous transmitter release. Neuron *29*, 197-208.

Filippi, A., Tiso, N., Deflorian, G., Zecchin, E., Bortolussi, M., and Argenton, F. (2005). The basic helix-loop-helix *olig3* establishes the neural plate boundary of the trunk and is necessary for development of the dorsal spinal cord. Proc. Natl. Acad. Sci. USA *102*, 4377-4382.

Fletcher, R.B., Watson, A.L., and Harland, R.M. (2004). Expression of *Xenopus tropicalis noggin1* and *noggin2* in early development: two *noggin* genes in a tetrapod. Gene Expr. Patterns *5*, 225-230.

Geering, K., Theulaz, I., Verrey, F., Häuptle, M.T., and Rossier, B.C. (1989). A role for the β-subunit in the expression of functional Na^+-K^+-ATPase in *Xenopus* oocytes. Am. J. Physiol. *257*, C851-C858.

Gloor, S., Antonicek, H., Sweadner, K.J., Pagliusi, S., Frank, R., Moos, M., and Schachner, M. (1990). The adhesion molecule on glia (AMOG) is a homologue of the β subunit of the Na,K-ATPase. J. Cell Biol. *110*, 165-174.

Gomez, T.M., Robles, E., Poo, M.-m., and Spitzer, N.C. (2001). Filopodial calcium transients promote substrate-dependent growth cone turning. Science *291*, 1983-1987.

Gomez, T.M., and Spitzer, N.C. (1999). *In vivo* regulation of axon extension and pathfinding by growth-cone calcium transients. Nature *397*, 350-355.

Good, P.J., Richter, K., and Dawid, I.B. (1990). A nervous system-specific isotype of the β subunit of the Na^+,K^+-ATPase expressed during early development of *Xenopus laevis*. Proc. Natl. Acad. Sci. USA *87*, 9088-9092.

Gorbunova, Y.V., and Spitzer, N.C. (2002). Dynamic interactions of cyclic AMP transients and spontaneous Ca^{2+} spikes. Nature *418*, 93-96.

Gottmann, K., Dietzel, I.D., Lux, H.D., and Rohrer, H. (1988). Development of inward currents in chick sensory and autonomic neuronal precursor cells in culture. J. Neurosci. *8*, 3722-3732.

Gu, X., Olson, E.C., and Spitzer, N.C. (1994). Spontaneous neuronal calcium spikes and waves during early differentiation. J. Neurosci. *14*, 6325-6335.

Gu, X., and Spitzer, N.C. (1993). Low-threshold Ca^{2+} current and its role in spontaneous elevations of intracellular Ca^{2+} in developing *Xenopus* neurons. J. Neurosci. *13*, 4936-4948.

Gu, X., and Spitzer, N.C. (1995). Distinct aspects of neuronal differentiation encoded by frequency of spontaneous Ca^{2+} transients. Nature *375*, 784-787.

Hasler, U., Wang, X., Crambert, G., Béguin, P., Jassier, F., Horisberger, J.-D., and Geering, K. (1998). Role of β-subunit domains in the assembly, stable expression, intracellular routing, and functional properties of Na,K-ATPase. J. Biol. Chem. *273*, 30826-30835.

Herrera, V.L.M., Cova, T., Sassoon, D., and Ruiz-Opazo, N. (1994). Developmental cell-specific regulation of Na^+-K^+-ATPase α_1-, α_2-, and α_3-isoform gene expression. Am. J. Physiol. *266*, C1301-C1312.

Hirsch, N., Zimmerman, L.B., and Grainger, R.M. (2002). *Xenopus*, the next generation: *X. tropicalis* genetics and genomics. Dev. Dyn. *225*, 422-433.

Holliday, J., Adams, R.J., Sejnowski, T.J., and Spitzer, N.C. (1991). Calcium-induced release of calcium regulates differentiation of cultured spinal neurons. Neuron *7*, 787-796.

Holliday, J., and Spitzer, N.C. (1990). Spontaneous calcium influx and its roles in differentiation of spinal neurons in culture. Dev. Biol. *141*, 13-23.

Ikeda, K., Onaka, T., Yamakado, M., Nakai, J., Ishikawa, T.-o., Taketo, M.M., and Kawakami, K. (2003). Degeneration of the amygdala/piriform cortex and enhanced fear/anxiety behaviors in sodium pump alpha2 subunit (Atp1a2)-deficient mice. J. Neurosci. *23*, 4667-4676.

Ikeda, K., Onimaru, H., Yamada, J., Inoue, K., Ueno, S., Onaka, T., Toyoda, H., Arata, A., Ishikawa, T.-o., Taketo, M.M.*, et al.* (2004). Malfunction of respiratory-related neuronal activity in Na^+, K^+-ATPase α2 subunit-deficient mice is attributable to abnormal Cl^- homeostasis in brainstem neurons. J. Neurosci. *24*, 10693-10701.

James, P.F., Grupp, I.L., Grupp, G., Woo, A.L., Askew, G.R., Croyle, M.L., Walsh, R.A., and Lingrel, J.B. (1999). Identification of a specific role for the Na,K-ATPase α2 isoform as a regulator of calcium in the heart. Mol. Cell *3*, 555-563.

Kessaris, N., Pringle, N., and Richardson, W.D. (2001). Ventral neurogenesis and the neuron-glial switch. Neuron *31*, 677-680.

Khokha, M.K., Chung, C., Bustamante, E.L., Gaw, L.W.K., Trott, K.A., Yeh, J., Lim, N., Lin, J.C.Y., Taverner, N., Amaya, E.*, et al.* (2002). Techniques and probes for the study of *Xenopus tropicalis* development. Dev. Dyn. *225*, 499-510.

Knöchel, S., Dillinger, K., Köster, M., and Knöchel, W. (2001). Structure and expression of *Xenopus tropicalis BMP-2* and *BMP-4* genes. Mech. Dev. *109*, 79-82.

Koizumi, K., Higashida, H., Yoo, S., Islam, M.S., Ivanov, A.I., Guo, V., Pozzi, P., Yu, S.-H., Rovescalli, A.C., Tang, D., and Nirenberg, M. (2007). RNA interference screen to identify genes required for *Drosophila* embryonic nervous system development. Proc. Natl. Acad. Sci. USA *104*, 5626-5631.

Komuro, H., and Rakic, P. (1992). Selective role of N-type calcium channels in neuronal migration. Science *257*, 806-809.

Komuro, H., and Rakic, P. (1993). Modulation of neuronal migration by NMDA receptors. Science *260*, 95-97.

Komuro, H., and Rakic, P. (1996). Intracellular Ca^{2+} fluctuations modulate the rate of neuronal migration. Neuron *17*, 275-285.

Laughery, M.D., Todd, M.L., and Kaplan, J.H. (2003). Mutational analysis of α-β subunit interactions in the delivery of Na,K-ATPase heterodimers to the plasma membrane. J. Biol. Chem. *278*, 34794-34803.

Lavoie, L., Levenson, R., Martin-Vasallo, P., and Klip, A. (1997). The molar ratios of α and β subunits of the Na^+-K^+-ATPase differ in distinct subcellular membranes from rat skeletal muscle. Biochemistry *36*, 7726-7732.

Lecuona, E., Luquín, S., Avila, J., García-Segura, L.M., and Martín-Vasallo, P. (1996). Expression of the β1 and β2 (AMOG) subunits of the Na,K-ATPase in neural tissues: cellular and developmental distribution patterns. Brain Res. Bull. *40*, 167-174.

Lescale-Matys, L., Putnam, D.S., and McDonough, A.A. (1993). Na^+-K^+-ATPase α1- and β1-subunit degradation: evidence for multiple subunit specific rates. Am. J. Physiol. *264*, C583-C590.

Lewis, R.S. (2007). The molecular choreography of a store-operated calcium channel. Nature *446*, 284-287.

Linnertz, H., Urbanova, P., Obsil, T., Herman, P., and Amler, E. (1998). Molecular distance measurements reveal an $(\alpha\beta)_2$ dimeric structure of Na^+/K^+-ATPase. J. Biol. Chem. *273*, 28813-28821.

Lockery, S., and Spitzer, N.C. (1992). Reconstruction of action potential development from whole-cell currents of differentiating spinal neurons. J. Neurosci. *12*, 2268-2287.

LoTurco, J.J., Owens, D.F., Heath, M.J., Davis, M.B., and Kriegstein, A.R. (1995). GABA and glutamate depolarize cortical progenitor cells and inhibit DNA synthesis. Neuron *15*, 1287-1298.

Louvi, A., and Artavanis-Tsakonas, S. (2006). Notch signalling in vertebrate neural development. Nat. Rev. Neurosci. *7*, 93-102.

Lu, Q.R., Sun, T., Zhu, Z., Ma, N., Garcia, M., Stiles, C.D., and Rowitch, D.H. (2002). Common developmental requirement for *olig* function indicates a motor neuron/oligodentrocyte connection. Cell *109*, 75-86.

Madan, P., Rose, K., and Watson, A.J. (2007). Na/K-ATPase β1 subunit expression is required for blastocyst formation and normal assembly of trophectoderm tight junction-associated proteins. J. Biol. Chem. *282*, 12127-12134.

Magyar, J.P., Bartsch, U., Wang, Z.-Q., Howells, N., Aguzzi, A., and Wagner, E.F. (1994). Degeneration of neural cells in the central nervous system of mice deficient in the gene for the adhesion molecule on glia, the β2 subunit of murine Na, K-ATPase. J. Cell Biol. *127*, 835-845.

Martín-Vasallo, P., Wetzel, R.K., García-Segura, L.M., Molina-Holgado, E., Arystarkhova, E., and Sweadner, K.J. (2000). Oligodendrocytes in brain and optic nerve express the β3 subunit isoform of Na,K-ATPase. Glia *31*, 206-218.

McCobb, D.P., Best, P.M., and Beam, K.G. (1989). Development alters the expression of calcium currents in chick limb motoneurons. Neuron *2*, 1633-1643.

McEwen, D.P., and Isom, L.L. (2004). Heterophilic interactions of sodium channel β1 subunits with axonal and glial cell adhesion molecules. J. Biol. Chem. *279*, 52744-52752.

McGrath, J., Somlo, S., Makova, S., Tian, X., and Brueckner, M. (2003). Two populations of node monocilia initiate left-right asymmetry in the mouse. Cell *114*, 61-73.

Messenger, E.A., and Warner, A.E. (1979). The function of the sodium pump during differentiation of amphibian embryonic neurones. J. Physiol. *292*, 85-105.

Messenger, N.J., and Warner, A.E. (2000). Primary neuronal differentiation in *Xenopus* embryos Is linked to the β3 subunit of the sodium pump. Dev. Biol. *220*, 168-182.

Mircheff, A.K., Bowen, J.W., Yiu, S.C., and McDonough, A.A. (1992). Synthesis and translocation of Na^+-K^+-ATPase α-and β-subunits to plasma membrane in MDCK cells. Am. J. Physiol. *262*, C470-C483.

Moseley, A.E., Lieske, S.P., Wetzel, R.K., James, P.F., He, S., Shelly, D.A., Paul, R.J., Boivin, G.P., Witte, D.P., Ramirez, J.M.*, et al.* (2003). The Na,K-ATPase α2 isoform is expressed in neurons, and its absence disrupts neuronal activity in newborn mice. J. Biol. Chem. *278*, 5317-5324.

Müller-Husmann, G., Gloor, S., and Schachner, M. (1993). Functional characterization of β isoforms of murine Na,K-ATPase. J. Biol. Chem. *268*, 26260-26267.

Nieuwkoop, P.D., and Faber, J. (1967). Normal table of *Xenopus laevis* (Daudin), 2nd edn (Amsterdam: North Holland Publishing Co.).

Noguchi, S., Higashí, K., and Kawamura, M. (1990). A possible role of the β-subunit of (Na,K)-ATPase in facilitating correct assembly of the α-subunit into the membrane. J. Biol. Chem. *265*, 15991-15995.

Noguchi, S., Mishina, M., Kawamura, M., and Numa, S. (1987). Expression of functional ($Na^+ + K^+$)-ATPase from cloned cDNAs. FEBS Lett. *225*, 27-32.

O'Brodovich, H., Staub, O., Rossier, B.C., Geering, K., and Kraehenbuhl, J.-P. (1993). Ontogeny of α_1- and β_1-isoforms of Na^+-K^+-ATPase in fetal distal rat lung epithelium. Am. J. Physiol. *264*, C1137-1143.

O'Dowd, D.K., Ribera, A.B., and Spitzer, N.C. (1988). Development of voltage-dependent calcium, sodium and potassium currents in *Xenopus* spinal neurons. J. Neurosci. *8*, 792-805.

Orlowski, J., and Lingrel, J.B. (1988). Tissue-specific and developmental regulation of rat Na,K-ATPase catalytic α isoform and β subunit mRNAs. J. Biol. Chem. *263*, 10436-10442.

Palma, V., Kukuljan, M., and Mayor, R. (2001). Calcium mediates dorsoventral patterning of mesoderm in *Xenopus*. Curr. Biol. *11*, 1606-1610.

Pu, H.X., Scanzano, R., and Blostein, R. (2002). Distinct regulatory effects of the Na,K-ATPase γ subunit. J. Biol. Chem. *277*, 20270-20276.

Raya, Á., Kawakami, Y., Rodríguez-Esteban, C., Ibañes, M., Rasskin-Gutman, D., Rodríguez-León, J., Büscher, D., Feijó, J.A., and Belmonte, J.C.I. (2004). Notch activity acts as a sensor for extracellular calcium during vertebrate left-right determination. Nature *427*, 121-128.

Root, C.M., Velázquez-Ulloa, N.A., Monsalve, G., Minakova, E., and Spitzer, N.C. (2008). Embryonically expressed GABA and glutamate drive electrical activity regulating neurotransmitter specification. J. Neurosci. *28*, 4777-4784.

Rowitch, D.H. (2004). Glial specification in the vertebrate neural tube. Nat. Rev. Neurosci. *5*, 409-419.

Sann, S.B., Xu, L., Nishimune, H., Sanes, J.R., and Spitzer, N.C. (2008). Neurite outgrowth and *in vivo* sensory innervation mediated by a $Ca_v2.2$-laminin β2 stop signal. J. Neurosci. *28*, 2366-2374.

Sarmah, B., Latimer, A.J., Appel, B., and Wente, S.R. (2005). Inositol polyphosphates regulate left-right asymmetry. Dev. Cell *9*, 133-145.

Schubiger, M., Feng, Y., Fambrough, D.M., and Palka, J. (1994). A mutation of the drosophila sodium pump α subunit gene results in bang-sensitive paralysis. Neuron *12*, 373-381.

Sedohara, A., Suzawa, K., and Asashima, M. (2006). Comparison of induction during development between *Xenopus tropicalis* and *Xenopus laevis*. Int. J. Dev. Biol. *50*, 385-392.

Shimojo, H., Ohtsuka, T., and Kageyama, R. (2008). Oscillations in Notch signaling regulate maintenance of neural progenitors. Neuron *58*, 52-64.

Shoshani, L., Contreras, R.G., Roldán, M.L., Moreno, J., Lázaro, A., Matter, K., and Cereijido, M. (2005). The polarized expression of Na^+,K^+-ATPase in epithelia depends on teh association between β-subunits located in neighboring cells. Mol. Bio. Cell *16*, 1071-1081.

Sive, H.L., Grainger, R.M., and Harland, R.M. (2000). Early development of *Xenopus laevis*: a laboratory manual (Cold Spring Harbor, New York: Cold Spring Harbor Laboratory Press).

Soboloff, J., Spassova, M.A., Tang, X.D., Hewavitharana, T., Xu, W., and Gill, D.L. (2006). Orai1 and STIM reconstitute store-operated calcium channel function. J. Biol. Chem. *281*, 20661-20665.

Spitzer, N.C. (2006). Electrical activity in early neuronal development. Nature *444*, 707-712.

Srinivasan, J., Schachner, M., and Catterall, W.A. (1998). Interaction of voltage-gated sodium channels with the extracellular matrix molecules tenascin-C and tenascin-R. Proc. Natl. Acad. Sci. USA *95*, 15753-15757.

Therien, A.G., Goldshleger, R., Karlish, S.J.D., and Blostein, R. (1997). Tissue-specific distribution and modulatory role of the γ subunit of the Na,K-ATPase. J. Biol. Chem. *272*, 32628-32634.

Tobin, V., Gouty, L.-A., Moos, F.C., and Desarménien, M.G. (2006). A store-operated current (SOC) mediates oxytocin autocontrol in the developing rat hypothalamus. Eur. J. Neurosci. *24*, 400-404.

Tsuda, T., Kaya, S., Yokoyama, T., Hayashi, Y., and Taniguchi, K. (1998). ATP and acetyl phosphate induces molecular events near the ATP binding site and the membrane domain of Na^+, K^+-ATPase. The tetrameric nature of the enzyme. J. Biol. Chem. *273*, 24339-24345.

Vagin, O., Tokhtaeva, E., and Sachs, G. (2006). The role of the β1 subunit of the Na,K-ATPase and its glycosylation in cell-cell adhesion. J. Biol. Chem. *281*, 39573-39587.

Vig, M., Peinelt, C., Beck, A., Koomoa, D.L., Rabah, D., Koblan-Huberson, M., Kraft, S., Turner, H., Fleig, A., Penner, R., and Kinet, J.-P. (2006). CRACM1 is a plasma membrane protein essential for store-operated Ca^{2+} entry. Science *312*, 1220-1223.

Wallingford, J.B., Ewald, A.J., Harland, R.M., and Fraser, S.E. (2001). Calcium signaling during convergent extension in *Xenopus*. Curr. Biol. *11*, 652-661.

Watts, A.G., Sanchez-Watts, G., Emanuel, J.R., and Levenson, R. (1991). Cell-specific expression of mRNAs encoding Na^+,K^+-ATPase α- and β-subunit isoforms within the rat central nervous system. Proc. Natl. Acad. Sci. USA *88*, 7425-7429.

Webb, S.E., and Miller, A.L. (2003). Calcium signalling during embryonic development. Nat. Rev. Mol. Cell Biol. *4*, 539-551.

Yaari, Y., Hamon, B., and Lux, H.D. (1987). Development of two types of calcium channels in cultured mammalian hippocampal neurons. Science *235*, 680-682.

Zhou, Q., and Anderson, D.J. (2002). The bHLH transcription factors olig2 and olig1 couple neuronal and glial subtype specification. Cell *109*, 61-73.

Zhou, Q., Choi, G., and Anderson, D.J. (2001). The bHLH transcription factor olig2 promotes oligodendrocyte differentiation in collaboration with nkx2.2. Neuron *31*, 791-807.